Symmetry everywhere

1

SYNOPSIS

- Symmetry in science and arts
- Visualizing symmetry
- Symmetry in everyday objects
- Defining symmetry
- Introducing symmetry notation

1.1 Introduction

When I was lecturing to chemistry students on crystal symmetry, I would usually begin with the question: 'what is common to the National Westminster Bank logo, a Mercedes-Benz car emblem and a molecule of 2,4,6-triazidotriazine?' Generally, there was no reply: maybe they banked at Lloyds, drove Fords and skipped the lectures on triazines—but when I showed a slide of these entities (Fig. 1.1) there was always someone who saw that it had something to do with the number 'three'. And that is a good way to begin the study of symmetry. Of course, it can all be done mathematically and there is a place for that, as will be shown in later chapters. But for the moment, a visual expression of symmetry will suffice. This chapter sets out to introduce ideas on symmetry, and to show that it is experienced by everyone in some way every day: breakfast at a table having reflection symmetry, a midday pint in a glass of cylindrical symmetry, an evening stroll with the Dalmatian—even no symmetry is a form of symmetry.

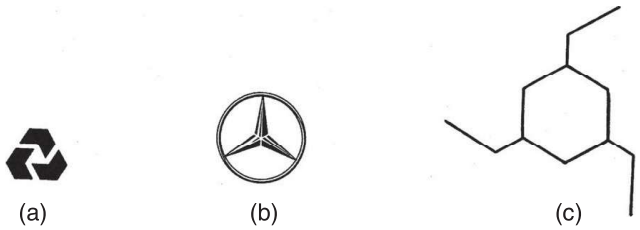

Fig. 1.1
(a) Logo of the National Westminster Bank. (b) Emblem of Mercedes-Benz cars. (c) Molecular skeleton of 2,4,6-triazidotriazine, $C_3N_3(N_3)_3$.

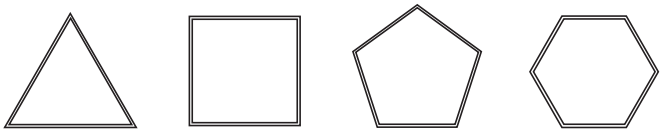

Fig. 1.2
Regular polygons.

1.2 Looking at symmetry

'"*Beauty is truth, truth beauty"—that is all ye know on earth, and all ye need to know*' [1]. Few of us have difficulty in recognizing symmetry in the plane geometrical shapes shown in Fig. 1.2. But it is a rather different matter when considering more complex three-dimensional objects (Fig. 1.3 and Fig. 1.4).

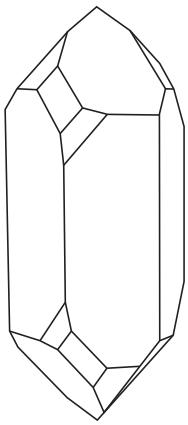

Fig. 1.3
Crystal of quartz, SiO_2.

Why should this be? I believe that the problem arises first from the fact that while one can see all parts of a two-dimensional object simultaneously, and thus take in the relationships of the parts to the whole, that cannot be done so easily in three dimensions. Secondly, although some three-dimensional objects, such as flowers, pencils and glass tumblers are simple enough to be rotated and examined visually, the natural gift for mentally perceiving and manipulating more complex objects may not be possessed by everyone. Nevertheless, the facility of doing so can be developed with suitable aids and with patience. If, initially, you have problems, take heart. You are not alone and, like many before you, you will be surprised at how swiftly the required facility can be acquired. Architects and sculptors may be blessed with a natural three-dimensional visualization aptitude, but they have learned to develop it—particularly by making and handling models.

Standard practice is always to reduce three-dimensional objects to two dimensions, in drawings such as projections and elevations: it is cheap, well suited to reproduction in books and less cumbersome than handling three-dimensional models. In this book, such two-dimensional representations still have a value, but to rely on them exclusively only delays the acquisition of a three-dimensional visualization ability. Fortunately, stereoscopic image pairs may be employed, such as that shown in Fig. 1.4. This type of illustration is a considerable help but, because it provides a view from only one standpoint, it is not always quite the equal of a model that can be examined by hand.

This illustration shows the crystal structure of oxalic acid dihydrate [2]. One half of the figure may be covered, whereupon the structure is viewed as a two-dimensional representation. Although the figure has been drawn carefully, with tapered bonds and hydrogen bonding indicated by double thin lines, it does not

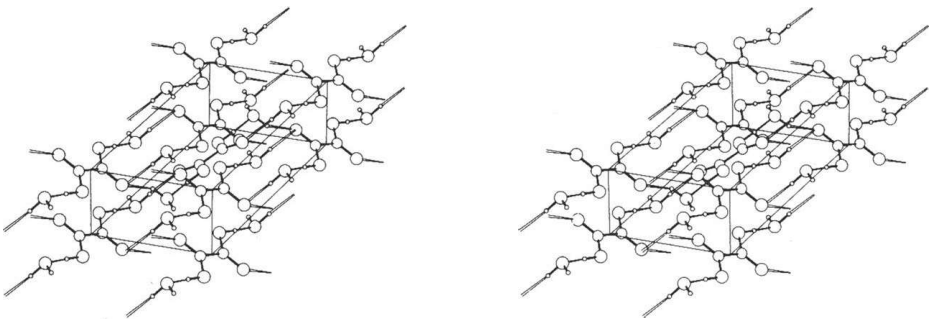

Fig. 1.4
Stereoview of the crystal structure of oxalic acid dihydrate, $(CO_2H)_2.2H_2O$; the circles in decreasing order of size represent O, C and H atoms. The double lines indicate hydrogen bonds, with the $H-O\cdots H$ bond distance of *ca.* 2.50 Å; the sum of the van der Waals radii for hydrogen and oxygen is 2.72 Å, which is good evidence of hydrogen bonding in this structure. [Reproduced by courtesy of Woodhead Publishing, UK.]

convey nearly as much information as the stereoview which, when viewed correctly, presents a convincing three-dimensional image. Notes on stereoviewers and stereoviewing are given in Appendix A1.

1.3 Some symmetrical objects

Four different objects are presented in Fig. 1.5. At first, there may not appear to be any connection between a Dobermann bitch, a Grecian urn, a molecule of 3-fluorochlorobenzene and a crystal of potassium tetrathionate. Yet each is an example of reflection symmetry: a symmetry plane (mirror plane, symbol *m*) can be imagined to divide each object into halves that are related

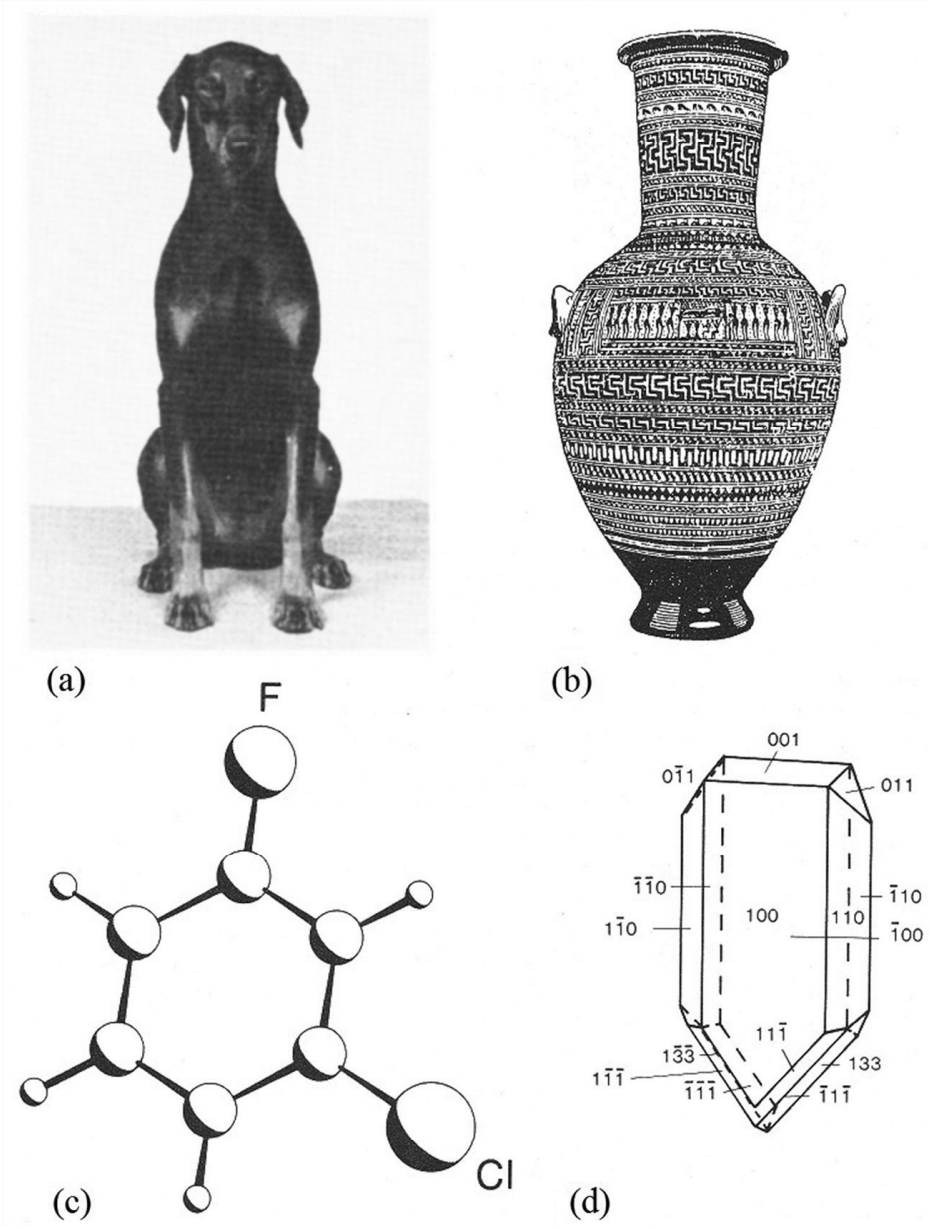

Fig. 1.5
Examples of reflection (mirror) symmetry. (a) Dobermann, *Vijentor Seal of Approval at Valmara*, JW. (b) Grecian urn. (c) Molecule of 3-chlorofluorobenzene; circles in decreasing order of size represent Cl, F, C and H atoms. (d) Crystal of potassium tetrathionate, $K_2S_2O_4$; with the crystal faces indexed by their Miller indices, (*hkl*). [Reproduced by courtesy of Woodhead Publishing, UK.]

Fig. 1.6
Portion of a floor with ideally square tiles.

exactly as an object is to its mirror image, like a right hand to its left hand. However, if the examples are perused in more detail, it would be noticed that the Dobermann bitch, beautiful animal that she is, does not have perfect *m* symmetry; the urn is not absolutely symmetrical; the molecule may not be totally planar; and the real crystal may have minute flaws that degrade perfect mirror symmetry.

In seeking symmetry around us, repeating patterns are soon encountered, such as tiled floors and brick walls (Fig. 1.6 and Fig. 1.7). Examine such structures in your locality at leisure, but do not be too critical about stains on the tiles or chips off the bricks. Perfect tiled floors and perfect brick walls are, like perfect crystals, conceptual. So what is the use of symmetry if the real objects that are to be studied are not strictly symmetrical?

The symmetry of objects can be studied both as finite bodies—the Grecian urn, the chemical molecule and as parts of larger, conceptually infinite bodies—the brick wall, the crystal. When investigating the internal structure of a crystal, which is one of the main reasons for studying crystal symmetry, it is discovered that a crystal of finite size is composed of a myriad of building blocks, or unit cells. Are all unit cells exactly alike? No; but to consider a specific case: sodium chloride crystallizes normally as cubes, and the basic unit of this crystal is also a cube, with an edge length of 0.564 nm[1] and volume of approximately 1.8×10^{-28} m^3.

Digressing for a moment: it is good practice to write numerical quantities as numbers from 0 to 9 with the appropriate 10^n multiplier; it makes for easy checks on calculations.

A crystal of sodium chloride of experimental size in an X-ray diffraction experiment could be of the order of 0.2, 0.2, 0.2 mm, a volume of 8×10^{-12} m^3. Thus, the number of unit cubes in the whole crystal is approximately 4×10^{16}. Symmetry concepts may be applied to real crystals because, although individual building units may exhibit sub-microscopic differences, the complete crystal behaves statistically towards physical observations as though it were perfect and infinite, and the results of treating the crystal in this way are found to be scientifically rewarding.

[1] 1 nm = 10 Å = 10^{-9} m

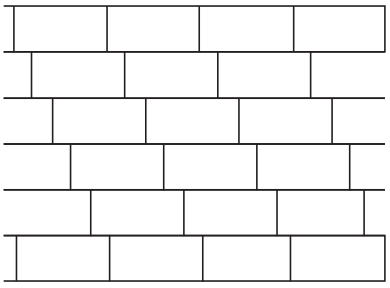

Fig. 1.7
Portion of a brick wall with ideally regular, rectangular bricks.

1.4 Defining symmetry

Symmetry is not an absolute property of a body: the result of a test for symmetry may depend on the nature of the examining probe. For example, the crystal structure of chromium appears different under X-ray and neutron diffraction examinations. Figure 1.8 illustrates the unit cell of chromium as seen both by X-rays and by neutrons. X-rays see a *body-centred* unit cell (a), but a neutron examination gives the different result, (b).

Elemental chromium has the electronic configuration $(Ar)(4s)^1(3d)^5$; it is antiferromagnetic below 38 °C and paramagnetic above this temperature. In the neutron diffraction experiment, although the individual atoms are similarly placed, magnetic interactions with the neutron beam reverse the direction of the magnetic moment of the central atom in the unit cell, so that it is no

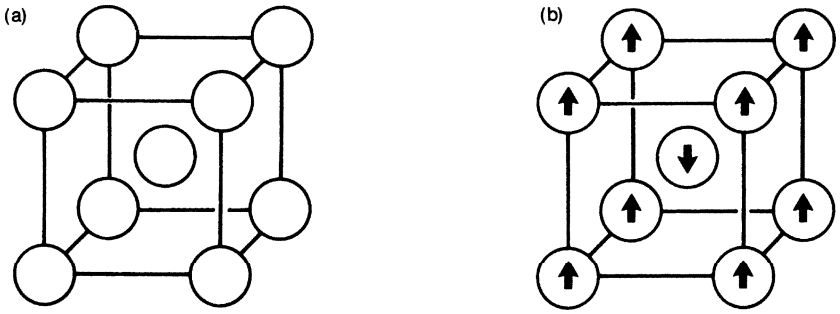

Fig. 1.8
Unit cell of the crystal structure of elemental chromium: (a) as seen by x-rays, and (b) as seen by neutrons; the arrows represent the direction of the magnetic moment vectors of the chromium atoms.

longer body-centred but *primitive*. Symmetry differences may arise also with optical and photoelastic properties.

This book will be concerned with the symmetry of the positional distribution of the parts of a molecule, crystal, body or pattern, as is revealed by visual inspection, microscopic examination or diffraction techniques. A definition of symmetry is *that spatial property of an assemblage by which the parts of the assemblage can be brought from an initial state to another indistinguishable state by means of a certain operation—a symmetry operation*. The term 'assemblage' is useful here because it can be used to describe the distribution of faces on a crystal, of bonds radiating from a central atom and of diffractions spectra from crystalline materials.

1.5 Symmetry in science

Manifestations of symmetry abound in most areas of science and, indeed, throughout nature; they are not confined to molecules and crystals. In botany, for example, the symmetry inherent in the structures of flowers and reproductive systems plays an important part in plant taxonomy. Figure 1.9 illustrates a white orchid, *Cattleya walkeriana*, var. *Alba*; its bilateral, or *m*, symmetry is clearly apparent.

Fig. 1.9
A bloom of the orchid *Cattleya walkeriana*, variation *Alba*, showing bilateral reflection symmetry. [Reproduced by courtesy of Greg Allikas.] (**See Plate 1**)

Examples of symmetry arise also in mathematics and physics. Consider first the equation

$$X^4 = 16 \tag{1.1}$$

Its roots are $X = \pm 2$ and $X = \pm 2\mathrm{i}$, where i is the square root of –1, and it may be seen immediately that these solutions have a symmetrical distribution about $X = 0$; the fourth power of each of these roots is 16.

The differential equation

$$\frac{\mathrm{d}^2 Y}{\mathrm{d}X^2} + k^2 Y = 0 \tag{1.2}$$

represents a type encountered, for example, in the physics of the simple pendulum or of a mass attached to a spring. Its general solution is

$$Y = A\exp(\mathrm{i}kX) + B\exp(-\mathrm{i}kX) \tag{1.3}$$

where A, B and k are constants. If reflection symmetry is introduced across the point $X = 0$, so that X is converted into $-X$, then the solution would become

$$Y = A\exp(-\mathrm{i}kX) + B\exp(\mathrm{i}kX) \tag{1.4}$$

Differentiating Eq. (1.4) twice with respect to X, shows that Eq. (1.4) is also a solution of Eq. (1.2). If a translation constant t is applied such that X becomes $X + t$, then again, the equation and its solution have similar symmetry properties.

The French mathematician and physicist Jean-Baptiste Joseph Fourier (1768–1830) solved problems on thermal conduction by means of a series consisting of cosine and sine terms [3]. Such series, termed Fourier series, are of fundamental importance in many areas of science. For example, in crystal structure analysis, X-ray diffraction data from a crystal structure are synthesized mathematically by Fourier summation to form an image of the electron density of the structure. A Fourier series is a single-valued, continuous, periodic function that can be represented by a series of cosine and sine terms. For a periodic, continuous function $Y(X)$, defined on the interval $\pm\pi$, the function may be formulated as the Fourier series

$$Y = A_0 + \sum_{\substack{k=-\infty \\ (k\neq 0)}}^{\infty} A_k \cos 2\pi kX + B_k \sin 2\pi kX \tag{1.5}$$

A typical cosine function, shown in Fig. 1.10, exhibits reflection symmetry about the line $X = 0$, and is an *even* function, $Y(-X) = Y(X)$. Contrast it with Fig. 1.11, a typical sine function, which shows inversion symmetry about the origin and is an *odd* function, $Y(-X) = -Y(X)$.

Example 1.1

Is the function $Y(X) = \sin X - X^3 \cos X$ even or an odd?

To answer this question, it is generally sufficient to consider the value of the function for a few values of X around the point $X = 0$. Thus, the table

X	*Y(X)*	*X*	*Y(X)*
–3	–26.8709	3	26.8709
–2	–4.23847	2	4.23847
–1	–0.301169	1	0.301169
0	0		

shows that the function is antisymmetric across the origin, which is indicative of an odd function.

Finally, in this section, consider a cube constructed from twelve 1 Ω resistors, as shown by Fig. 1.12. Let an electrical current I be set up across the points A and G. What would be the effective resistance of this assembly of resistors for the path of the current from A to G? The problem is simplified by considering the symmetry of the cube: the planes $ACGE$ (broken lines), $AFGD$ and $BGHA$ are all mirror planes, of the type already discussed. Thus, the currents flowing along AB, AD, AE, CG, FG and HG are all equal to $I/3$.

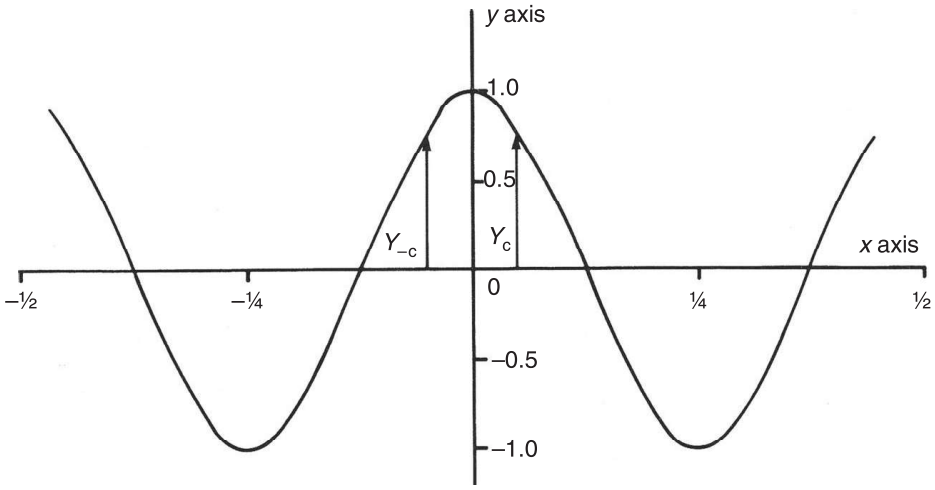

Fig. 1.10
Graph of an even function, $f(-X) = f(X)$: $Y = \cos 2\pi kX$, $k = 2$; $-1/2 \leq X \leq 1/2$.

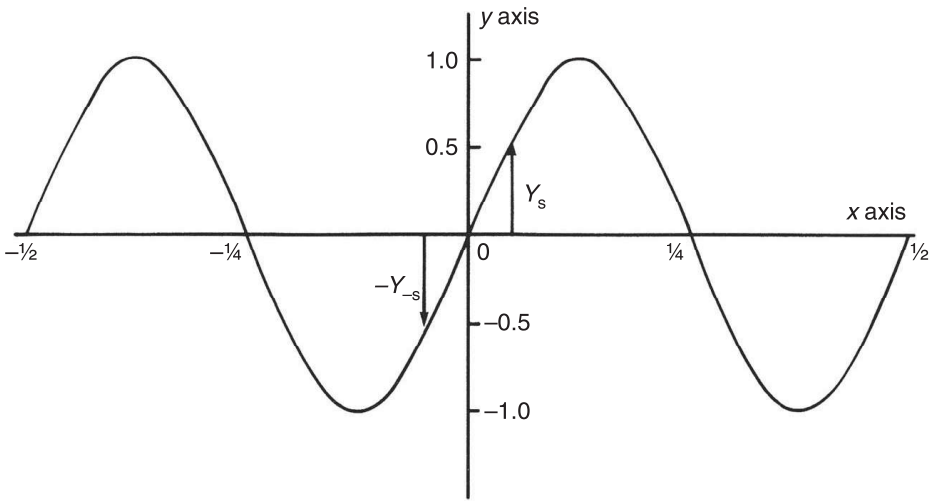

Fig. 1.11
Graph of an odd function, $f(-X) = -f(X) : Y = \sin 2\pi kX$, $k = 2$; $-1/2 \leq X \leq 1/2$.

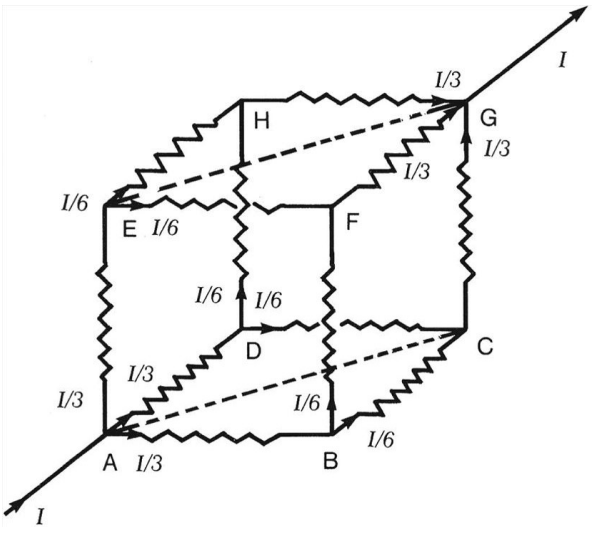

Fig. 1.12
Cubic network of 1Ω resistors; electric current I flows through the resistors from A to G.

The m symmetry requires that the currents in EF and EH are equal, and each current here is $I/6$. Similarly, the currents in BC and DC are also $I/6$, from which it follows that those in BF and DH are $I/6$. Hence, any path through the assembly of resistors from A to G has an effective resistance of 5/6 Ω.

1.6 Symmetry in music

Symmetry has featured in music from Bach to Bartók and beyond, an early example being the so-called *Crab Canon* from Bach's *Musical Offering*, which was written in a palindromic form, such that its second part is the same as the first part but written backwards (*see* Problem 1.11). Figure 1.13 illustrates an extract from the well-known classic, *Étude* No. 12, Opus 10 by Chopin, which shows approximate reflection symmetry, whereas the opening bars of Beethoven's piano sonata in C sharp minor, Opus 27, No. 2, '*Moonlight*' (Fig. 1.14) is an illustration of translational symmetry. Of course, music has to progress and to end, so that true translational symmetry is not possible. Often the symmetry in music is apparent rather than true, but can be discovered in many forms [4]. Even the piano itself exhibits an example of symmetry (Fig. 1.15).

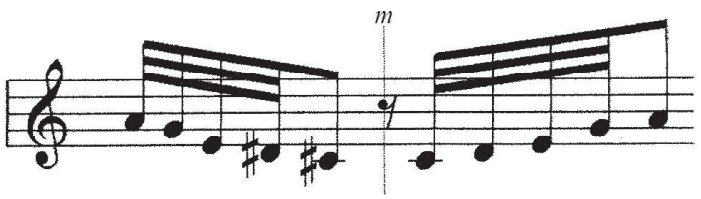

Fig. 1.13
Reflection symmetry in music: an extract from *Étude* No. 12, Opus 10, by Chopin; the thin line marked m is an approximate reflection line.

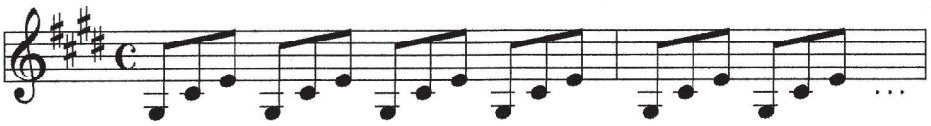

Fig. 1.14
Opening bars of Beethoven's '*Moonlight*' sonata; an example of translational symmetry, though not of infinite extent.

Fig. 1.15
Symmetry of the piano keyboard; the keys of the triads A–C and E–G are symmetrical about the key D.

1.7 Symmetry in architecture

Architecture of all cultural periods has made extensive use of symmetry. As there are many kinds of symmetry, so many kinds of architecture have evolved. A type of symmetry is chosen so as to achieve a particular objective in terms of beauty and utility. Unlike most other arts, architecture has spatiality. While two-dimensional composition is relatively straightforward, in three dimensions there is a greater call on the imagination. The symmetry of an object is fixed but the perception of it changes with the relative position of the observer. One can not only move around but also through architectural designs, thus providing experiences of symmetry.

Architectural elements comprise solid and void components, and an architectural body may be characterized by the nature of its elements and their symmetry. Thus, differing types of symmetry occur in architecture, but there is space here to consider only a few of them.

Reflection symmetry is probably the most common architectural form (Fig. 1.16). Rotation symmetry occurs in domes, and cylindrical symmetry exists in towers and columns; even spherical symmetry occurs, as in Boullée's *Cenotaph for Isaac Newton*, projected but never brought to fruition. Chiral

Fig. 1.16
Bilateral symmetry of the Parthenon; the Greeks avoided placing the reflection line on a pillar by having an even number of pillars.

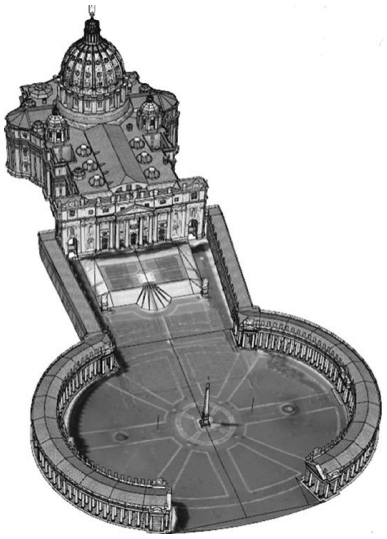

Fig. 1.17
Model of Bernini's St. Peter's Colonnade. [Reproduced by courtesy of its author, Enrico Dalbosco; <http://www.enricodalbosco.it>] (**See Plate 2**)

symmetry makes use of design based on mirror images, and is well illustrated by St. Peter's Colonnade (Fig. 1.17).

Whereas the above examples reflect point group symmetry, translational symmetry in architecture is a pseudo space group symmetry, but it falls seriously short of the ideal as its manifestations in rows of pillars or arches of viaducts are of very limited extent,.

1.8 Summary and notation

Symmetry, then, is a feature that is encountered in both scientific and everyday life. In the following chapters, crystals and molecules will be studied first as finite, non-repeating bodies, and then the expression of symmetry through symmetry functions and point groups will be developed. Subsequently, the symmetry of ideally infinite patterns will be examined, together with their application to crystal structures. On the basis of the understanding of symmetry so gained, it is complementary to discuss the mathematical approach of group theory and its applications. A brief encounter with black–white and colour symmetry will also be presented.

It may seem that the important application of symmetry in chemistry has been overlooked in this introduction. However, this topic will be effectively addressed through the work of several of the subsequent chapters, as the study of symmetry is pursued. But first a word about notation.

1.8.1 Introducing symmetry notation

There exist two notations for describing symmetry, both of which are in common use. The Hermann–Mauguin notation [5,6] is highly mnemonic, and desirable in the description of crystals and crystal structures. For work with molecules, the Schönflies notation [7] is also in general use; with space groups, however, this notation is less elegant and has little to recommend it in that application. The Hermann–Mauguin, or international, notation will be used at first; when the principles of symmetry have been grasped, there should be little problem with an alternative symmetry notation.

References 1

[1] Keats J. *Ode on a Grecian urn*. 1820.
[2] Ahmed FR and Cruickshank DWJ. *Acta Crystallogr*. 1953; 6: 385.
[3] Fourier J-BJ. *Théorie analytique de la chaleur*, Firmin, Didot [first published in 1822]. Cambridge, UK: Cambridge University Press, 2009.
[4] Dorrell P. *What is music?: solving a scientific mystery*. <http://whatismusic.info/> (2006).
[5] Hermann C. *Z. Kristallogr*. 1928; 68: 257; ibid. 69: 226; ibid. 69: 533; ibid. 76: 559.
[6] Mauguin C. *Z. Kristallogr*. 1931; 76: 542.
[7] Schönflies AM. *Krystallsysteme und Krystallstruktur*. Leipzig, 1891.

Problems 1

1.1 Seek out the following objects in the home, or elsewhere, and list their mirror symmetry. (a) Plain teacup. (b) Plain rectangular table. (c) Outer sleeve of a matchbox, ignoring the label. (d) Plain building brick. (e) Inner tray of a matchbox, ignoring colour. (f) Gaming die.

1.2 Study the patterns of Fig. 1.6 and Fig. 1.7, considering them to be extended. Illustrate each pattern by a minimum number of representative points.

1.3 Twelve identical 1 Ω resistors are connected so as to form a regular octahedron. Use the symmetry of the octahedron, which is the same as that of the cube, to evaluate its effective resistance to an electrical current between any pair of opposite apices.

1.4 Consider Fig. 1.5c. (a) What single atom change would double the number of *m* planes in the molecule? (b) Where do the planes lie in the more symmetrical molecule?

1.5 Write in upper case those letters of the alphabet that cannot exhibit *m* symmetry across a line. Your answer may depend on how you form the letters.

1.6 State whether the following functions of X have even or odd symmetry.
(a) X^3 (b) $\sin^2 X$ (c) $\cos^3(X)$ (d) $X^1 \sin X$ (e) $X^3 - X$ (f) $X \cos X$

1.7 Try out the Symmetry Game to be found at the following website: <http://www.innovationslearning.co.uk/subjects/maths/activities/year3/symmetry/shape_game.asp>.

1.8 Refer to Fig. 1.2. (a) Find the number of *m* lines in each of these figures. (b) Name the figures. (c) Deduce a relationship between the number *n* of the sides of a polygon and the number *M* of symmetry lines that it presents? (c) Why does a rectangle not follow the rule so derived?

1.9 Figure. P1.1 shows two views of the C–H bond directions in the molecule of ethane, C_2H_6, as seen in a Newman projection; the C–C bond lies normal to the plane of the diagram. What differences are there in reflection symmetry in these two conformations?

1.10 Consider the parabola $Y = (X + 3)^2 - 4$. Determine the position of the vertical symmetry line of the parabola.

1.11 Figure. P1.2 shows a portion of Bach's *Musical Offering* (*Crab Canon*). What symmetry exists in this extract of music?

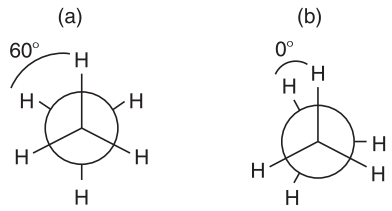

Fig. P1.1
Newman projections of the molecule of ethane, C_2H_6: (a) staggered, (b) eclipsed. The dihedral angle is 60° for (a) and 0° for (b); in the latter diagram, a twist of a few degrees has been applied to the C–C bond in order to make the eclipsed hydrogen atom apparent. The eclipsed form is approximately 12 kJ mol^{-1} higher in energy (less stable) than the staggered form.

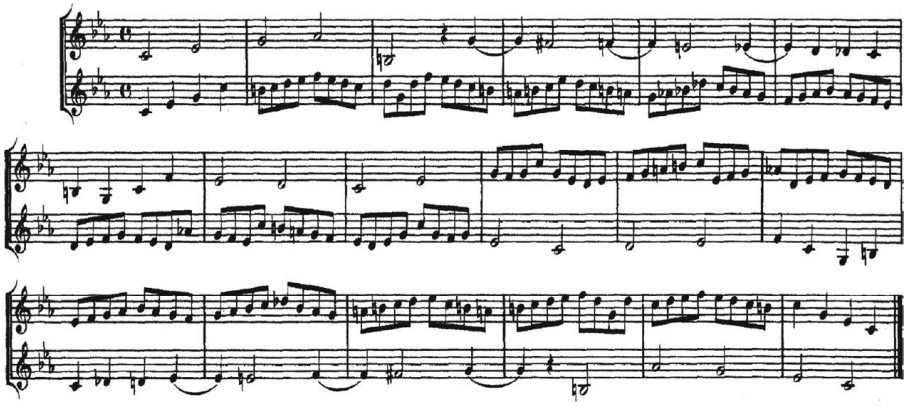

Fig. P1.2
Portion of Bach's *Musical Offering* (*The Crab Canon*).

1.12 What aspects of symmetry are evident in the illustration of the Taj Mahal?

Fig. P1.3
The Taj Mahal.

Lattices

4

SYNOPSIS

- Lattices in one, two and three dimensions
- Unit cell and asymmetric unit
- Lattices in the seven crystal systems
- Law of rational intercepts
- Introduction to the reciprocal lattice
- Rotational symmetry of lattices
- Lattice transformations
- Wigner–Seitz cells

4.1 Introduction

The next logical step is the examination of the internal structure of crystals, so their basis, the three-dimensional lattices or Bravais lattices, forms the next topic. The Bravais lattices may be approached by considering first lattices in fewer dimensions. In any dimension, a lattice may be defined as *a regular arrangement of points in space*, *of infinite extent*, *such that each point has the same environment as every other point*. Key words here are 'regular', 'infinite', 'environment' and 'point'. The essence of most crystalline solids is regularity, whether in one dimension or more, and a lattice is ideally of infinite extent. That a practical use can be made of an infinite concept follows from the discussion in Section 1.2, and the identical environment of each point ensures the regularity of the pattern built up by the lattice. It is necessary to remember that a lattice is an arrangement of mathematical points: they are joined up, as in children's early drawing books, so as to form a picture, in this case one that allows a ready appreciation of the geometry of the lattice.

4.2 One-dimensional lattice

In order to begin an appreciation of lattices, consider Fig. 4.1a; it is a line of identical, regular bricks placed exactly end-to-end. A fixed point can be identified at the same location on each brick, and so a series of points is

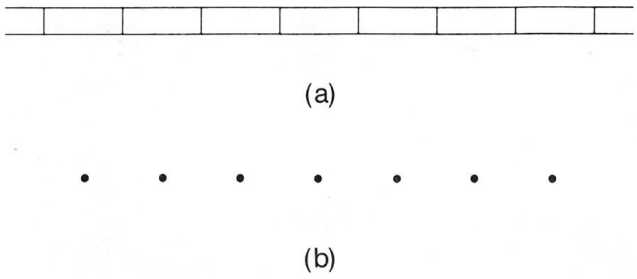

Fig. 4.1
Simulation of a one-dimensional lattice, or *row*. (a) Series of identical bricks placed end-to-end. (b) Line of representative mathematical points forming a one-dimensional lattice; the points relate to the same position on the bricks.

Table 4.1 Symmetry and dimensionality of lattices.

	Dimension		
Symmetry operation	**One (*Row*)**	**Two (*Net*)**	**Three (*Bravais*)**
Reflection	Across a point	Across a line	Across a plane
Rotation	–	About a point	About a line
Inversion	–	–	In a point

defined, representative of the row of bricks: this series of points represents a one-dimensional lattice, or *row*, and the points form a regular, ideally infinite pattern, each point in the same environment as every other point.

In considering the number of lattices, the number of *different arrangements* of points is needed whatever the dimension under consideration: in one dimension, there is only a single lattice, and the only lattice symmetry is that of reflection across any point. The argument in Section 3.5 on the extension of symmetry operations with increased dimensionality may be recalled here; for convenience, the results are summarized in Table 4.1.

4.3 Two-dimensional lattices

If the construction of bricks in Fig. 4.1a is extended to two dimensions, in the traditional manner, a brick wall (Fig. 4.2a) results. As before, each brick can be represented by a point, placed at the same location in each brick, and so build up a two-dimensional lattice, or *net*. Fig. 4.2b is a stack of rows, in this example each row is translated by one half row spacing with respect to successive rows.

A general net is shown in Fig. 4.3. It is convenient to represent the net by a *unit cell*, such as that outlined by vectors **a** and **b** in cell I. The net can be

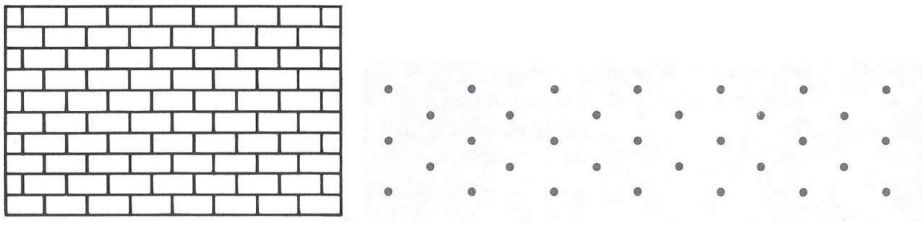

Fig. 4.2
Simulation of a two-dimensional lattice, or *net*. (a) Wall formed by stacking bricks of Figure 4.1a in the traditional manner. (b) Two-dimensional lattice: the points represent the same location on the bricks.

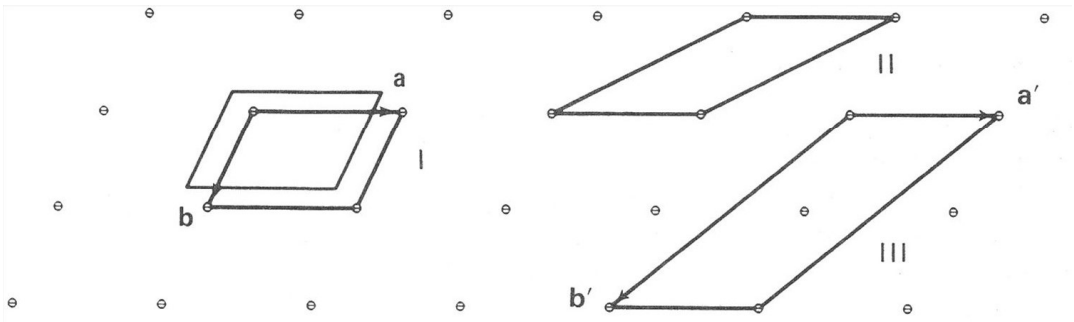

Fig. 4.3
Oblique net: I (conventional unit cell), II and III are three of an infinite number of possible unit cells; I and II are primitive, *p*, and III is centred, *c*. [Reproduced by courtesy of Springer Science+Business Media, New York, © Kluwer Academic/Plenum Publishing.]

then constructed by stacking unit cells side-by-side, in the same orientation and sharing adjacent lattice points. The unit cell I is *primitive*, symbol *p*: each lattice point is associated with the area of one unit cell. This fact may be appreciated either by noting that each point is shared equally by four unit cells, or by translating the unit cell framework by a small distance, as shown by the thin lines in cell I.

Every lattice point is a position of point group symmetry. In one dimension, the symmetry at each point is *m*. In a net, each point has the symmetry of one of the ten two-dimensional point groups (Section 3.4ff). It is desirable not to refer to a unit cell by a point group symbol, because a unit cell is representative of an infinite array of points and, therefore, not truly describable by point group symmetry.

4.3.1 Choice of unit cell

The choice of unit cell is to some extent arbitrary. Three unit cells are shown in Fig. 4.3. The conventional choice is the smallest sized repeat unit, provided that the vectors delineating that unit cell lie on or are parallel to important symmetry directions in the lattice. Thus, a conventional unit cell such as **a**, **b**, in Fig. 4.4b is not always the smallest in its lattice.

4.3.2 Nets in the oblique system

The possible nets are referred conveniently to the two-dimensional systems discussed in Section 3.4.4. In unit cell I (Fig. 4.3), $a \not\in b$ and γ, the angle $\angle\mathbf{ab}$, is $\not\in 90°$ or 120°; angles of these values *in a lattice* would lead to higher symmetry; the symbol $\not\in$ should be read as '*not constrained by symmetry to equal*'. Unit cell II has the same area as cell I, but has a more obtuse, less convenient γ angle. The *centred* unit cell *c* is clearly twice as large as I or II, and would not be chosen. It does not represent a new oblique lattice, as the following transformation shows:

$$\mathbf{a} = \mathbf{a}' \tag{4.1}$$

$$\mathbf{b}' = \frac{\mathbf{a}'}{2} + \frac{\mathbf{b}'}{2} \tag{4.2}$$

The result is not unexpected, since a lattice is invariant under choice of unit cell.

4.3.3 Nets in the rectangular system

If a, b or γ is specialized in a non-trivial manner, the symmetry at each lattice point will be then greater than 2: a condition such as $a' = 2a$ is trivial, and does not lead to a new arrangement of points.

Consider the net in Fig. 4.4a: the symmetry at each point is $2mm$, and the net is allocated to the rectangular system. Three possible unit cells are outlined, of which cell I is the conventional choice (Section 4.3.1). Unlike in the oblique system, the centred cell **a, b** here forms a new arrangement of points (Fig. 4.4b). The primitive unit cell $\mathbf{a}'$, $\mathbf{b}'$ is a true unit cell in this net, and is of smaller area. It is not the conventional choice because, in isolation, it does not show clearly the lattice symmetry. The symmetry is still present, as can be inferred from the transformation equations:

$$\left.\begin{aligned} \mathbf{a}' &= \frac{\mathbf{a}}{2} - \frac{\mathbf{b}}{2} \\ \mathbf{b}' &= \frac{\mathbf{a}}{2} + \frac{\mathbf{b}}{2} \end{aligned}\right\} \tag{4.3}$$

whence

$$a' = b' = \left(\frac{a^2}{4} + \frac{b^2}{4}\right) \tag{4.4}$$

Thus, a parallelogram unit cell with equal sides, a rhombus, in a lattice has symmetry $2mm$ at each lattice point: the value of γ', the angle between $\mathbf{a}'$ and $\mathbf{b}'$, depends on the ratio $\frac{a}{b}$.

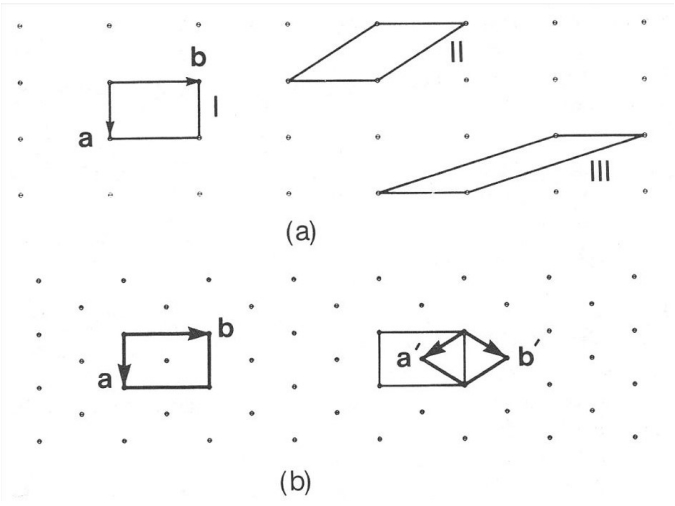

Fig. 4.4
Rectangular nets. (a) In the conventional p unit cell I, **a** and **b** are parallel to the m symmetry lines; p cells II and III both have the same area as I, but neither is simply related to the m lines. (b) A centred c unit cell **a**, **b** is the conventional choice here; the p cell $\mathbf{a}'$, $\mathbf{b}'$, although of smaller area, is oblique to the m symmetry lines and is not the conventional choice. [Reproduced by courtesy of Springer Science+Business Media, New York, © Kluwer Academic/Plenum Publishing.]

4.3.4 Square and hexagonal nets

Increased specialization in the unit cell parameters leads to nets in the square and hexagonal systems, which will be addressed in Problem 4.1; the five two-dimensional lattices are listed in Table 4.2.

The honeycomb arrangement of points in Fig. 4.5a is not a lattice because the environment of all points is not identical. A true net may be formed by centring the honeycomb: but then each centred honeycomb cell encompasses three primitive (triply primitive) hexagonal unit cells. If one of these primitive cells itself were now centred, the arrangement would no longer represent a hexagonal net: from the above discussion, the symmetry would be degraded to $2mm$ and the net rectangular.

Table 4.2 The five two-dimensional lattices.

System	Unit cell symbol	Point symmetry	Unit cell parameters
Oblique	p	2	$a \not\in b;\ \gamma \not\in 90°, 120°$
Rectangular	p, c	$2mm$	$a \not\in b; \gamma = 90°$
Square	p	$4mm$	$a = b; \gamma = 90°$
Hexagonal	p	$6mm$	$a = b; \gamma = 120°$

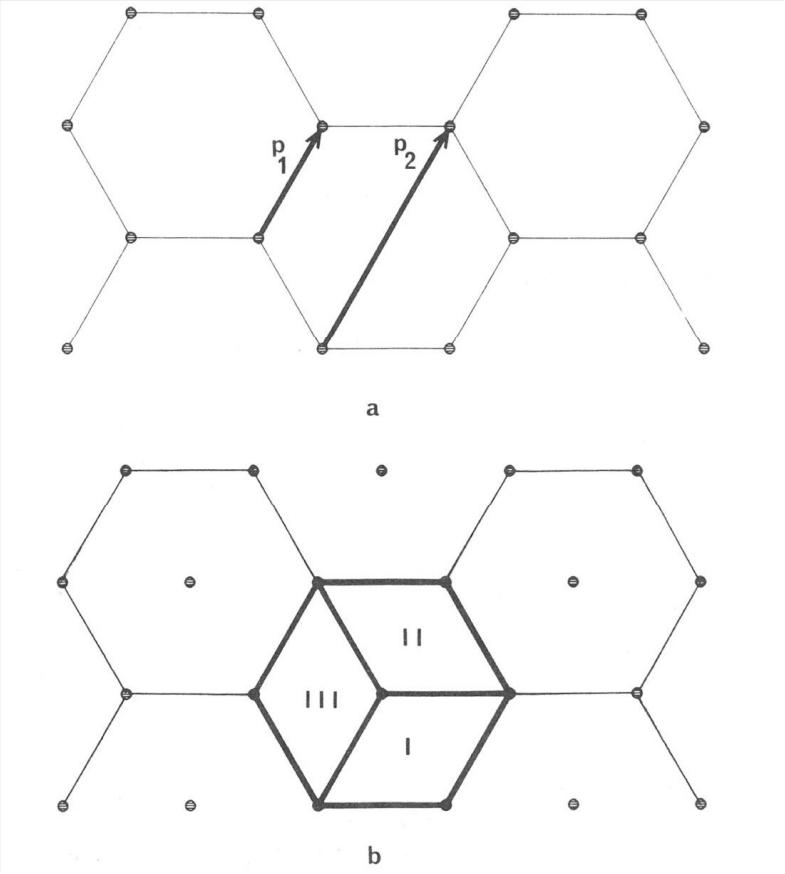

Fig. 4.5
The honeycomb arrangement of points is not a lattice; compare the environment of points $\mathbf{p}_1$ and $\mathbf{p}_2$. (b) True lattice, but now with three p unit cells within the centred hexagon. [Reproduced by courtesy of Springer Science+Business Media, New York, © Kluwer Academic/Plenum Publishing.]

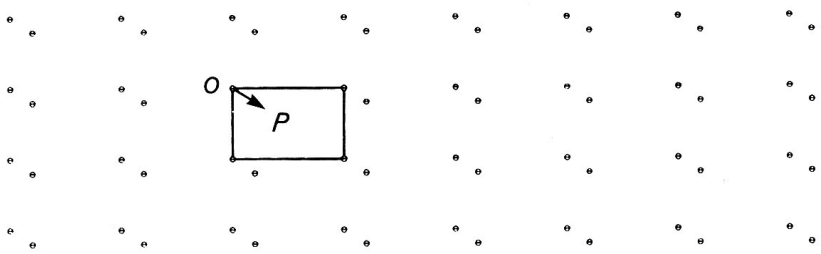

Fig. 4.6
A rectangular net, with two lattice points in the *p* unit cell. Only if all points have the same vector environment can they form a true lattice. Thus, the only position is the centre of the cell, to give a *c* unit cell (see also Section 4.4.6). [Reproduced by courtesy of Woodhead Publishing, UK.]

4.3.5 Unit cell centring

The centred unit cells described here have a lattice point at their geometrical centre. That this is the only site for a centring point in a lattice is clear from Fig. 4.6: if a point were placed at *P*, then an identical vector placed at that point would not terminate on another lattice point. This illustration is a rectangular primitive net with two points per unit cell; alternatively, it could be described as two identical primitive nets superimposed with a vector translation **OP**. There is an exception to this rule, as will emerge with hexagonal and trigonal lattices, in Section 4.4.6 and Section 4.4.7, respectively.

4.4 Three-dimensional lattices

'If you have to fill a volume with a structure that's repetitive, just keep your wits about you, you don't need to take a sedative! Don't freeze with indecision, there's no need for you to bust a seam! Although the options may seem endless, really there are just fourteen' [1]. But Frankenheim found 15 [2]! However, Bravais determined that two of Frankenheim's lattices referred to monoclinic *C* [3,4]; thus, the designation *Bravais* lattice is in general use.

Section 4.1 introduced the lattice as the geometrical basis for crystal structure, and gave a definition of it that continues to be applicable in three dimensions. If a number of nets (Section 4.3) is aligned in a regular manner at a spacing *c*, non-collinear with *a* or *b*, a three-dimensional lattice is obtained; Fig. 4.7 shows a stereoview of such a lattice. The fourteen Bravais

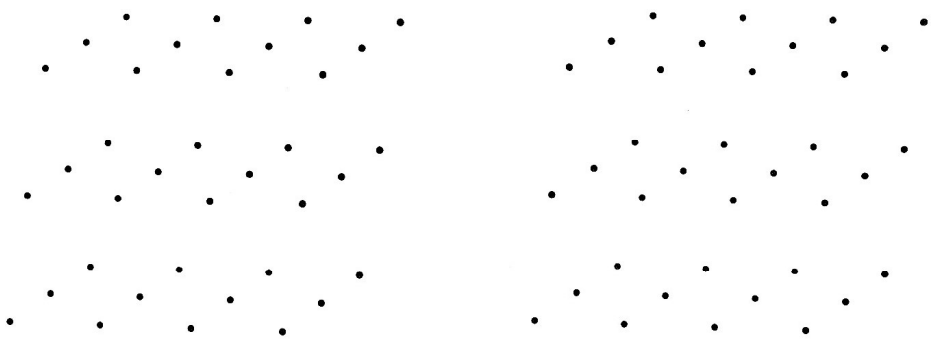

Fig. 4.7
Stereoview of a three-dimensional lattice, obtained by stacking nets at a regular spacing, non-collinear with the spacings of the net. [Reproduced by courtesy of Woodhead Publishing, UK.]

lattices are distributed unequally among the seven crystal systems according to their symmetry. A unit cell for each lattice is chosen in the conventional manner (Section 4.3.1) and thus is not always primitive. The lattices in the seven crystal systems will be studied, beginning with the least symmetrical.

4.4.1 Triclinic lattice

The triclinic lattice is illustrated in Fig. 4.8. The unit cell is characterized by the parameters $a \not= b \not= c$ and $\alpha \not= \beta \not= \gamma \not= 90°, 120°$. Similar conditions were given in Table 3.4 for the intercepts of the parametral plane and the interaxial angles, arising from purely morphological considerations.

There is only one triclinic lattice, and its conventional unit cell is primitive, symbol P (upper case letters in three dimensions): it contains one lattice point per unit cell and the symmetry at each lattice point is $\bar{1}$; any centred triclinic cell can be reduced to a primitive triclinic cell.

When the unit cell parameters are specialized in a non-trivial manner, higher symmetry always results, and other crystal systems revealed.

4.4.2 Monoclinic lattices

The symmetry at each lattice point in the monoclinic system is $2/m$, and the conventional unit cell takes the standard conditions $a \not= b \not= c$, $\alpha = \gamma = 90° \not= \beta$, with β chosen to be obtuse. The variable angle β corresponds to the characteristic twofold symmetry axis parallel to the y axis. In all systems where the unit cell has a typically non-specialized value of a parameter, it is always possible that it may exhibit an uncharacteristic value. Thus, some monoclinic crystals have been shown to have a β angle that is 90° within the limits of experimental measurement: but they remain monoclinic, because the symmetry of the crystal is dictated by the arrangement of the contents of the unit cell.

In three dimensions, there are several types of centring possible for the Bravais lattices, as set out in Table 4.3 with their standard notation. The table lists also the *fractional coordinates* of the centring points.

Fractional coordinates are dimensionless quantities: the fractional coordinate x is defined as X/a, where X and a represent, respectively, the coordinate in

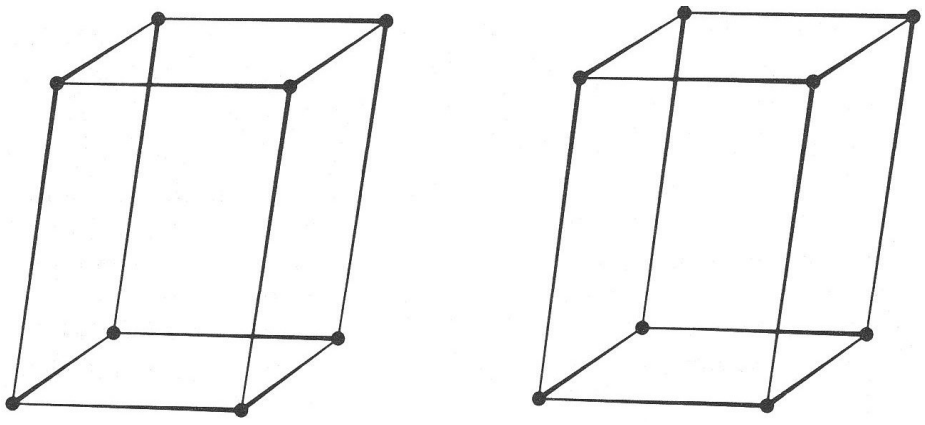

Fig. 4.8
Stereoview of a P unit cell in the triclinic lattice. In the illustrations of unit cells herein, the origin is in the bottom left, rear corner, with $+a$ towards the reader, $+b$ to the right and $+c$ upward. The parameters of the conventional unit cells are listed in Table 4.4 (Cp. Table 3.4). [Reproduced by courtesy of Woodhead Publishing, UK.]

Table 4.3 Notation for unit cells of the Bravais lattices.

Centring site/s in the unit cell	Symbol	Miller indices of centred faces	Fraction coordinates of unique lattice points
None	P, R	—	0, 0, 0
	R_{hex}[a]	—	0, 0, 0; 1/3, 2/3, 2/3; 2/3, 1/3, 1/3
b, c faces	A	(100)	0, 0, 0; 0, 1/2, 1/2
c, a faces	B	(010)	0, 0, 0; 1/2, 0, 1/2
a, b faces	C	(001)	0, 0, 0; 1/2, 1/2, 0
Body	I	—	0, 0, 0; 1/2, 1/2, 1/2
All faces	F	(100), (010) (001)	0, 0, 0; 0, 1/2, 1/2; 1/2, 0, 1/2; 1/2, 1/2, 0

[a] The points $\pm(1/3, 2/3, 2/3)$ in R_{hex} are as a form of centring.

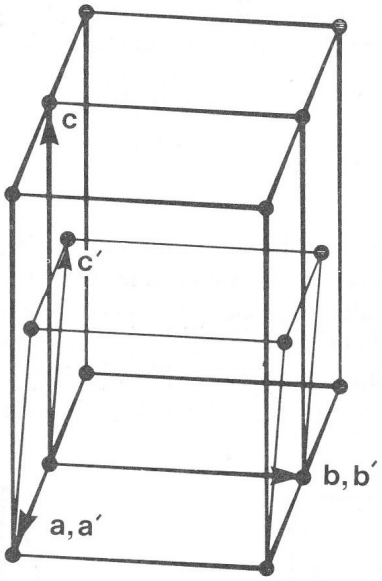

Fig. 4.9
Monoclinic lattice showing two B centred unit cells, **a**, **b**; the conventional P unit cell **a**′, **b**′ is outlined. [Reproduced by courtesy of Woodhead Publishing, UK.]

absolute measure and the corresponding unit cell dimension in the same units; similar definition apply for y and z. They have the obvious advantage of being independent of the dimensions of the unit cell.

Centring the B faces of a monoclinic unit cell is illustrated in Fig. 4.9. In this case another unit cell can be defined by the transformation:

$$\left.\begin{aligned} \mathbf{a}' &= \mathbf{a} \\ \mathbf{b}' &= \mathbf{b} \\ \mathbf{c}' &= -\frac{\mathbf{a}}{2} + \frac{\mathbf{c}}{2} \end{aligned}\right\} \tag{4.5}$$

The choice of $-\mathbf{a}/2$ in $\mathbf{c}'$ instead of $\mathbf{a}/2$ is often necessary in the monoclinic system, so as to ensure the standard convention that β' is oblique. Now, $a' \not\perp b' \not\perp c'$; and since c' lies in the a', c' plane, $\alpha' = \gamma' = 90°$ but β' is still a general value, consistent with monoclinic symmetry. The transformed unit cell is P and has half the volume of the B cell, as can be seen by counting the lattice points *per unit cell*, and is the conventional choice.

A C unit cell in a monoclinic lattice is shown in stereoview in Fig. 4.10, neglecting the thin lines for the moment. An A centred unit cell does not represent a different monoclinic lattice, because the x and z axes can interchanged, while retaining b as the unique twofold symmetry direction, provided that the signs of the directions of the x and z axes are set so as to preserve a right-handed axial set.

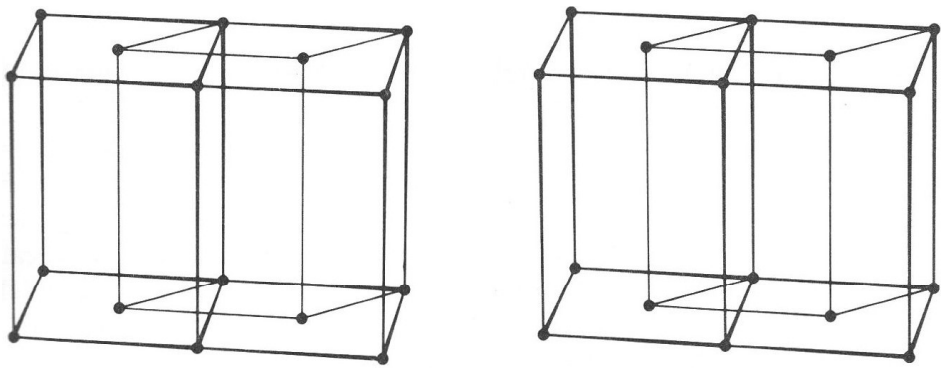

Fig. 4.10
Stereoview of two monoclinic C unit cells; the P cell outlined is not the conventional choice for this lattice.

So far, the conditions $A \equiv C$ and $B \equiv P$ have been deduced. A different result is obtained if the C unit cell is transformed to P, as shown by the thin lines in Fig. 4.10. A transformation is given by

$$\left.\begin{aligned} \mathbf{a}' &= \frac{\mathbf{a}}{2} - \frac{\mathbf{b}}{2} \\ \mathbf{b}' &= \mathbf{b} \\ \mathbf{c}' &= \mathbf{c} \end{aligned}\right\} \tag{4.6}$$

Now $a' \not\perp b' \not\perp c'$ and $a' = 90°$. However, because the a, b plane is inclined to the b, c plane, γ', as well as β', is different from 90°. These results indicate that monoclinic C is different from monoclinic P in the arrangement of points, so that both descriptors are relevant to this system. Monoclinic I and F unit cells both transform to C, and further discussion of them will be given in the Problems section of this chapter. In carrying out these transformations, it is always necessary to retain both the right-handed system of axes, and, as far as is practicable, an obtuse value for the β angle.

Example 4.1 Practical transformations involve numerical computation. In the transformation $B \rightarrow P$ given by Eq. (4.5), only c' and β' need be calculated.

From the discussion in Appendix A3.2.2, it follows that

$$\begin{aligned} \mathbf{c}' \cdot \mathbf{c}' &= \left(-\frac{\mathbf{a}}{2} + \frac{\mathbf{c}}{2}\right) \cdot \left(-\frac{\mathbf{a}}{2} + \frac{\mathbf{c}}{2}\right) \\ c'^2 &= \frac{a^2}{4} + \frac{c^2}{4} - \frac{ac\cos\angle\mathbf{ac}}{2} \\ c' &= \left(\frac{a^2}{4} + \frac{c^2}{4} - \frac{ac\cos\beta}{2}\right)^{1/2} \end{aligned} \tag{4.7}$$

and

$$\begin{aligned} &\mathbf{a}' \cdot \mathbf{c}' = a'c'\cos\beta' \\ &\cos\beta' = \mathbf{a} \cdot \left(\frac{-\mathbf{a}/2 + \mathbf{c}/2}{ac'}\right) = \frac{1}{ac'}\left(\frac{-a^2}{2} + \frac{ac\cos\beta}{2}\right) \\ &\beta' = \cos^{-1}\left(\frac{-a + c\cos\beta}{2c'}\right) \end{aligned} \tag{4.8}$$

4.4.3 Orthorhombic lattices

The symmetry at a lattice point being that of the appropriate Laue group implies that the point symmetry is *mmm* in any orthorhombic lattice. In the conventional unit cell, $a \not\perp b \not\perp c$ and $\alpha = \beta = \gamma = 90°$. Unit cells P, C, I and F exist for this system. The A-centred and B-centred orthorhombic unit cells can always be transformed to orthorhombic C: in studying space groups, however, A-centring is also required; in such cases, the equivalence of A and B still applies. Fig. 4.11 illustrates a body-centred orthorhombic unit cell. That the P, C, I and F cells represent different orthorhombic arrangements can be demonstrated, following the procedure used with the monoclinic $B \rightarrow P$ transformation:

After centring a P unit cell, the following questions should be considered, in order:

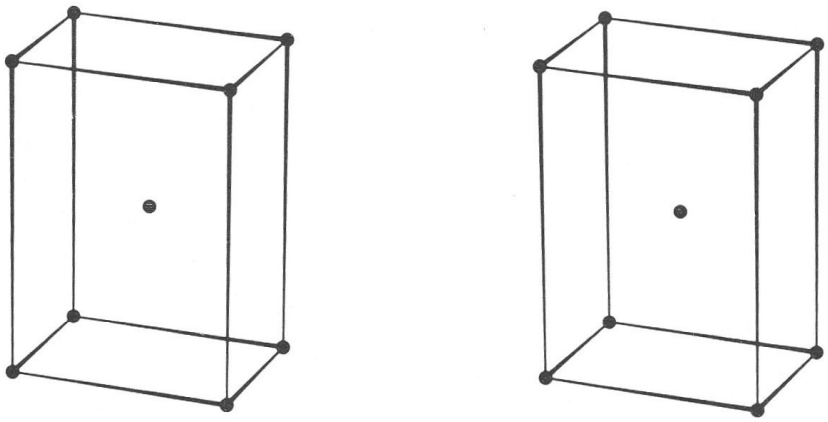

Fig. 4.11
Stereoview of the orthorhombic *I* unit cell.

- Does the centred cell represent a true lattice?
- If it is a lattice, is the symmetry of the unit cell drawing apparently different from that of the *P* cell?
- If the symmetry is unchanged, does the centred cell represent a different arrangement of points? It may be judged by comparing the parameters of the two cells in question, which is equivalent to asking if the unit cell has been chosen according to convention.

These questions have been answered implicitly in the monoclinic transformations already studied.

The correct number of lattices can be reached in another way. The orthorhombic system is characterized by three axes, 2 or $\bar{2}$, along a, b and c. From the matrices in Appendix A3.7.1, a twofold rotation of a vector $\mathbf{r}(x, y, z)$ about the axis along a has the effect $x\mathbf{a}$, $y\mathbf{b}$, $z\mathbf{c} \rightarrow x\mathbf{a}$, $\bar{y}\mathbf{b}$, $\bar{z}\mathbf{c}$; similarly, a rotation of the same initial vector about the axis along b has the effect $x\mathbf{a}$, $y\mathbf{b}$, $z\mathbf{c} \rightarrow \bar{x}\mathbf{a}$, $y\mathbf{b}$, $\bar{z}\mathbf{c}$. From the study of point groups, it is evident that the changes in sign show that **a** is perpendicular to **b** and **c**, and that **b** is perpendicular to **c** and **a**. The product of the matrices for these two operations is a matrix that has the effect $x\mathbf{a}$, $y\mathbf{b}$, $z\mathbf{c} \rightarrow \bar{x}\mathbf{a}$, $\bar{y}\mathbf{b}$, $z\mathbf{c}$. Thus, the three twofold axes are mutually perpendicular, as was found earlier, in Section 3.6.3.

Conditions such as this can be confirmed in another way. The scalar product from the first transformation: $x\mathbf{a} \cdot y\mathbf{b} \rightarrow x\mathbf{a} \cdot (-y\mathbf{b})$ or $xyab \cos\gamma \rightarrow -xyab \cos\gamma$. Since the twofold symmetry operation leads to indistinguishability, $xyab \cos\gamma = -xyab \cos\gamma$, or $2 \cos\gamma = 0$, which shows that γ is 90°. By considering the product $x\mathbf{a} \cdot z\mathbf{c}$, β is found also to be 90°. If the product $y\mathbf{b} \cdot z\mathbf{c}$ in the first transformation be examined, it evolves as $yzbc \cos\alpha = (-y)(-z)bc \cos\alpha$. This reveals nothing about the angle α, because this transformation concerns only the b, c plane. However, when the argument is applied to the second transformation, α is found to be 90°. Also, since there has been no interchange among the x, y and z coordinates during these transformations, there can be no restriction on the values of a, b and c. Thus, the arrangement of twofold axes determines a system in which $a \neq b \neq c$ and $\alpha = \beta = \gamma = 90°$, and is called orthorhombic. Hence, any reduction of a centred unit cell that infringes conditions so deduced shows that the centred cell is proper to its system. Try it for the monoclinic *C* cell example (Fig. 4.10). In the crystal

systems, the conditions impinging on the conventional unit cells on account of the characteristic symmetry (Table 3.4) can all be deduced in this way.

4.4.4 Tetragonal lattices

There are two tetragonal lattices, symmetry $\frac{4}{m}mm$ at each point, represented by P and I unit cells; their parameters are: $a = b \not\in c$; $\alpha = \beta = \gamma = 90°$. It is straightforward to show that $C \equiv P$ and $F \equiv I$.

Consider centring the B faces: the unit cell no longer has the characteristic tetragonal symmetry. The symmetry is restored, apparently, by centring the A faces as well. But this arrangement is not a lattice, as Fig. 4.12 shows. Centring now the C faces produces a true tetragonal F unit cell, but this is equivalent to I, and is not a new lattice (Fig. 4.13).

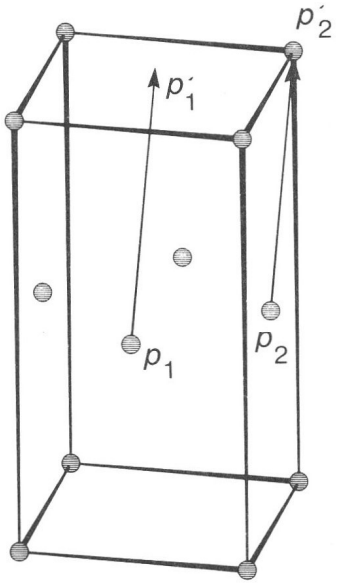

Fig. 4.12
A 'tetragonal' unit cell centred on the A and B faces does not represent a lattice, because of the differing environments of $\mathbf{p}_1$ and $\mathbf{p}_2$.

4.4.5 Cubic lattices

There are three cubic lattices, P, I and F, consistent with $m\bar{3}m$ symmetry at each point and unit cell parameters $a = b = c; \alpha = \beta = \gamma = 90°$. If the A faces are centred (Fig. 4.14a), the symmetry of the lattice is reduced $m\bar{3}\ m \rightarrow mmm$. If a cubic I cell is transformed by the equations

$$\left.\begin{aligned} \mathbf{a}' &= \mathbf{a} \\ \mathbf{b}' &= \mathbf{b} \\ \mathbf{c}' &= \mathbf{a} + \mathbf{c} \end{aligned}\right\}$$

the new cell is A centred, apparently monoclinic in isolation, and unconventional. However, it still has cubic symmetry as it represents the same lattice (Fig. 4.14b): the symmetry is inherent in the special conditions $a' = b'$, $c' = a'\sqrt{2}, \alpha = \gamma = 90°, \beta' = 45°$.

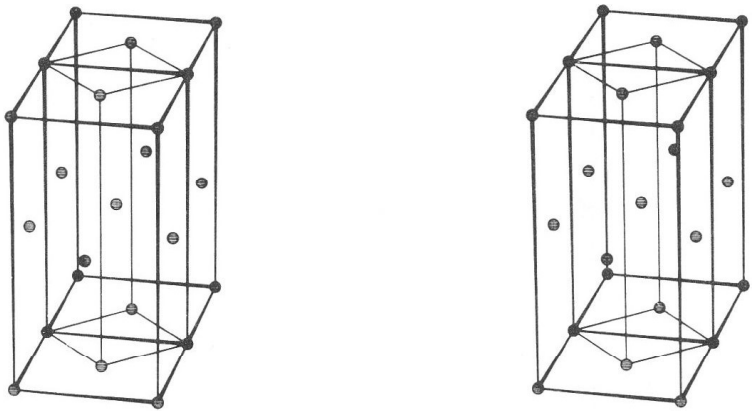

Fig. 4.13
Stereoview of a tetragonal lattice, showing the equivalence of F and I unit cells.

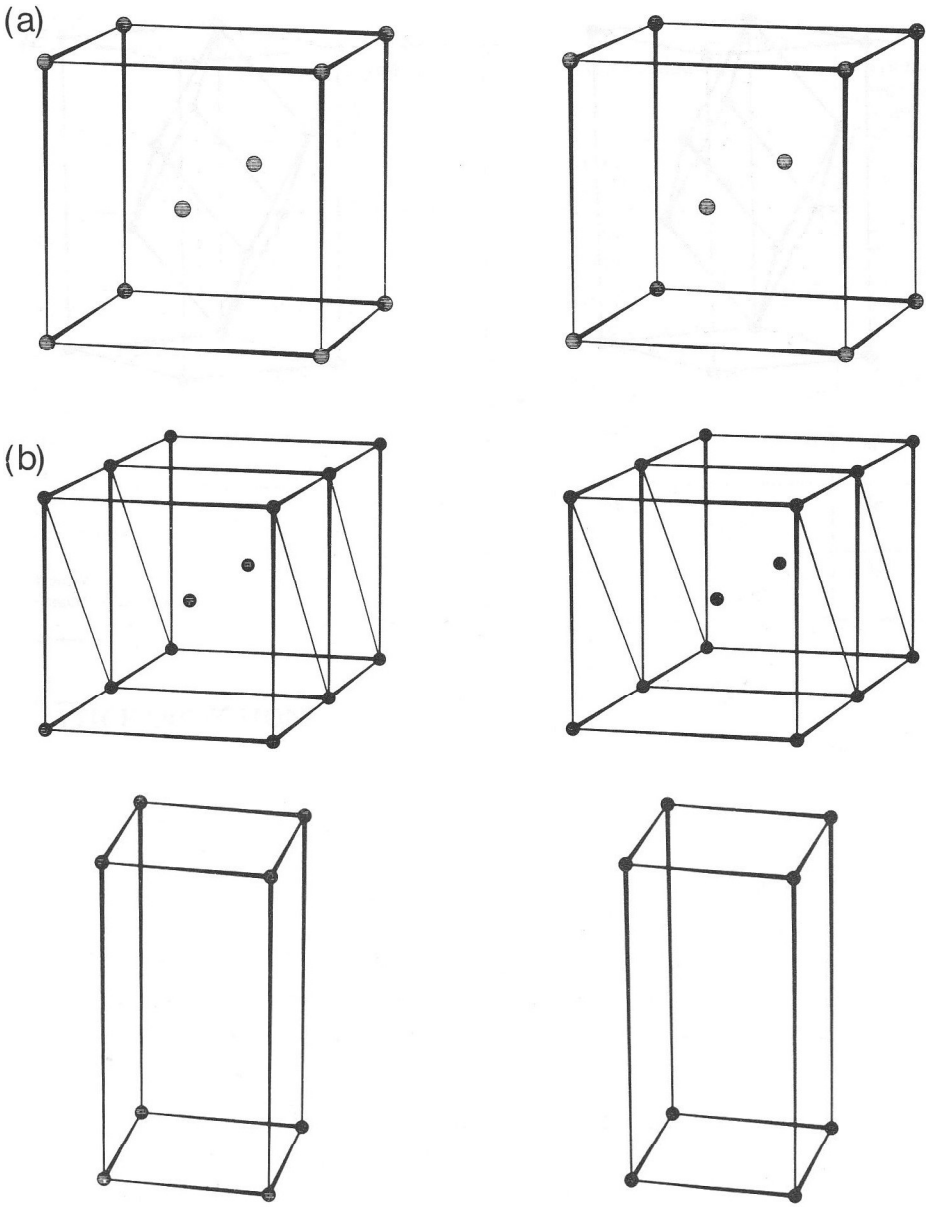

Fig. 4.14
(a) Stereoview of a cubic P unit cell degraded to orthorhombic A by centring the A faces alone. (b) Cubic I: the thin lines delineate another unit cell, with $a' = b' \not\in c', \alpha = \gamma = 90^{\circ}, \beta = 45^{\circ}$, apparently monoclinic C, but the symmetry at each point remains $m\bar{3}\,m$, so that it is a non-standard representation of the cubic lattice.

Fig. 4.15
Stereoview of a P unit cell in the hexagonal lattice.

4.4.6 Hexagonal lattice

The hexagonal lattice has a P unit cell, with $a = b \not\in c; \alpha = \beta = 90^{\circ}, \gamma = 120^{\circ}$; the lattice has point symmetry $\frac{6}{m}mm$, as shown in Fig. 4.15. If the hexagonal unit cell is centred as C, I or F, it is no longer hexagonal. Check this for yourself by drawing, or otherwise. However, if the 'centring' is carried out in the sense of base centring the two trigonal prisms that make up the hexagonal unit cell, that is, at the points $\pm(\frac{1}{3}, \frac{2}{3}, 0)$, then the hexagonal symmetry is retained, and a smaller hexagonal unit cell is obtained:

$$|\mathbf{a}'| = |\tfrac{1}{3}\mathbf{a} + \tfrac{2}{3}\mathbf{b}|; \quad |\mathbf{b}'| = |-\tfrac{1}{3}\mathbf{a} + \tfrac{1}{3}\mathbf{b}|; \ \mathbf{c}' = \mathbf{c},$$

whence $a' = b' = a\sqrt{3}/3$ and $\gamma' = 120^{\circ}$, and a new lattice is not formed. Show that the volume of the 'new' cell is one third that of the 'old' cell.

Another valid lattice is obtained if the hexagonal unit cell is 'centred' at $\pm(^2/_3, ^1/_3, ^1/_3)$, which introduces the trigonal lattice.

4.4.7 Trigonal lattices

A hexagonal unit cell is compatible with sixfold and threefold symmetry, and the centring just discussed leads to a lattice in the trigonal system (Fig. 4.16). The lattice no longer has the characteristic 6 or $\bar{6}$ symmetry of the hexagonal system. It is for this reason that the Schönflies point group symbol for $\bar{6}\,m2$ is C_{3h}, and the comment in Section 3.10.2, that the symmetry $\bar{6}$ cannot operate on a rhombohedral lattice should be now clear. Since this trigonal lattice has threefold symmetry axes parallel to z and passing through points with x, y coordinates $^2/_3, ^1/_3$ and $^1/_3, ^2/_3$, the possibility of a triply primitive hexagonal H cell exists. Thus, for some trigonal crystals the unit cell is P, whereas for others it will be R_{hex}, which can be deduced from the systematic absences in an X-ray diffraction record (see Fig. 5.36).

The R_{hex} cell can be transformed to the primitive rhombohedral cell R, for which $a = b = c$ and $\alpha = \beta = \gamma \neq 90°$ and $< 120°$. In this R cell, the

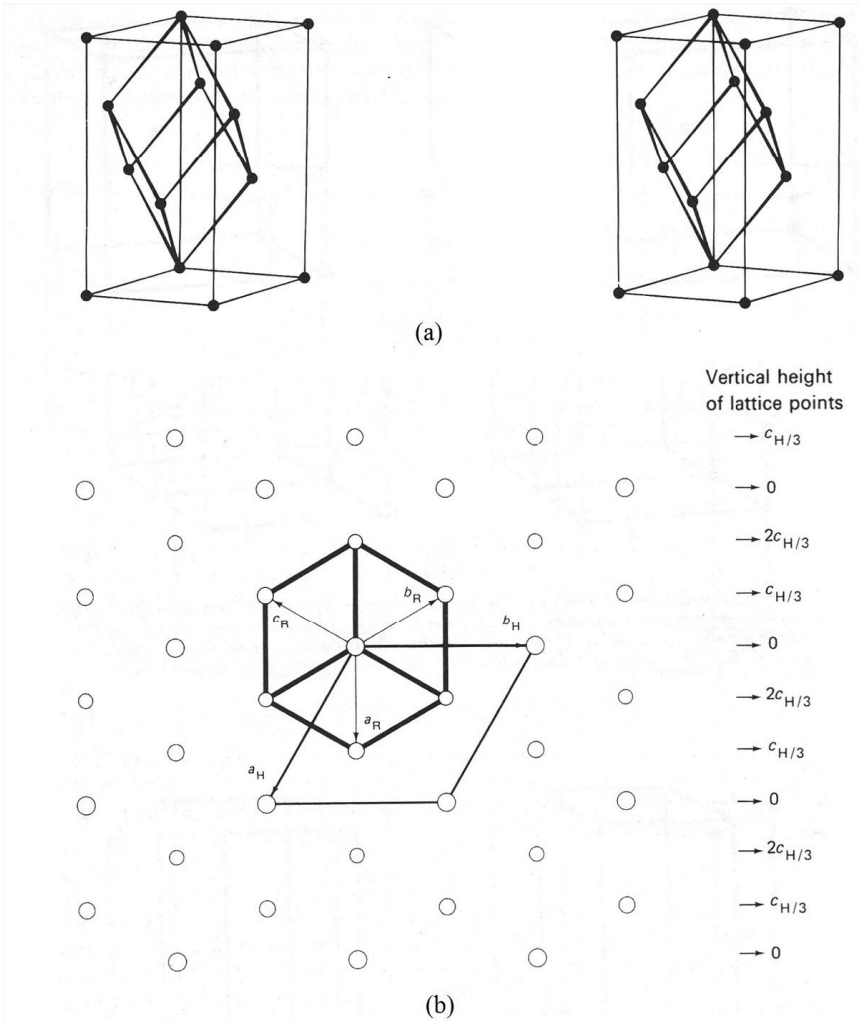

Fig. 4.16
(a) Stereoview of the rhombohedral (trigonal) R unit cell in the *obverse* setting with respect to a hexagonal unit cell. (b) Rhombohedral lattice and R unit cell, $\mathbf{a}_R, \mathbf{b}_R, \mathbf{c}_R$, viewed along [111]. The outlined hexagon delineates the triply primitive hexagonal unit cell, $\mathbf{a}_H, \mathbf{b}_H, \mathbf{c}_H$, and the fractions in the right-hand column refer to heights along z; $\mathbf{c}_H$ is normal to the $\mathbf{a}_H, \mathbf{b}_H$ plane and passes through the origin.

threefold axis is along [111], and its volume takes the simpler expression $V = \sqrt{a^3(1 - 3\cos^2\alpha + 2\cos^3\alpha)}$. The lattice that is represented by a conventional R unit cell is the single, true, trigonal unit cell. A cube extended or compressed along its [111] direction produces a rhombohedral unit cell; in compression it remains trigonal, but the α angle would be greater than 180° and therefore unconventional.

There are two settings of the R cell in relation to the hexagonal cell: the *obverse* setting, shown in Fig. 4.16, and the *reverse* setting, obtained by rotating the R cell clockwise about c_H by 60°; the obverse setting is standard.

It is worth noting that symbols such as P and C do not actually describe lattices, although they are used in this way. A lattice is an infinite array of points, each of the same symmetrical environment. Whether or not it is termed P, C or other designation depends on how the array is viewed, in other words, how the unit cell is chosen. Hence, a designation C, for example, implies that a choice of unit cell type has been made for a particular lattice: other choices are possible in the same lattice, although they are not necessarily conventional [5]. As long as terms such as 'P lattice' and 'C lattice' are used with this proviso, the practice is acceptable. The Bravais lattice data are summarized in Table 4.4.

4.5 Lattice directions

Lattice geometry is based around the three unit cell translation vectors **a**, **b** and **c**. From the definition of lattice, it follows that any point may be reached,

Table 4.4 The Bravais lattice unit cells.

System	Unit cell symbols	Axial relationships[a]	Symmetry[b] at each lattice point
Triclinic	P	$a \not= b \not= c$ $\alpha \not= \beta \not= \gamma \not= 90°,\ 120°$	$\bar{1}$
Monoclinic (y unique)	P, C	$a \not= b \not= c$ $\alpha = \gamma = 90°,\ \beta \not= 90°,\ 120°$	$2/m$
Orthorhombic	P, C, I, F	$a \not= b \not= c$ $\alpha = \beta = \gamma = 90°$	mmm
Tetragonal	P, C	$a = b \not= c$ $\alpha = \beta = \gamma = 90°$	$\frac{4}{m}mm$
Cubic	P, I, F	$a = b = c$ $\alpha = \beta = \gamma = 90°$	$m\bar{3}\,m$
Hexagonal	P	$a = b \not= c$ $\alpha = \beta = 90°, \gamma = 120°$	$\frac{6}{m}mm$
Trigonal (Hexagonal axes)	P	$a = b \not= c$ $\alpha = \beta = 90°, \gamma = 120°$	$\bar{3}\,m$
Trigonal (Rhombohedral axes)	R	$a = b = c$ $\alpha = \beta = \gamma \not= 90°, < 120°$	$\bar{3}\,m$

[a] Read ≠ as 'not constrained by symmetry to equal'.
[b] A lattice point exhibits the highest symmetry of its system.

starting from any other point, by performing the basic translations, or positive or negative multiples thereof, always in the directions of **a**, **b** and **c**.

Any lattice point may be taken as an origin for the lattice; then, the vector **r** to any other lattice point is given by

$$\mathbf{r} = U\mathbf{a} + V\mathbf{b} + W\mathbf{c} \tag{4.9}$$

where U, V and W are positive or negative integers or zero, and are the *coordinates* of the lattice point. The line joining the origin to the lattice points U, V, W; $2U$, $2V$, $2W$; $\ldots nU, nV, nW$ defines the *direction*, or *directed line*, $[UVW]$. The notation here is similar to that used for zone axes, because a direction, as defined here, is a possible zone axis, since crystal planes are rational. A set of directions related by symmetry defines a form of directions, signified by the notation $<UVW>$.

In a similar way, any general position in the unit cell has fractional coordinates x, y and z. Hence, the vector **d** from the origin of the unit cell to the point x, y, z is given by

$$\mathbf{d} = x\mathbf{a} + y\mathbf{b} + z\mathbf{c} \tag{4.10}$$

The numerical values of **r** and **d** can be evaluated from their scalar products, $\mathbf{d} \cdot \mathbf{d}$ and $\mathbf{r} \cdot \mathbf{r}$, following Appendix A3.2.1.

Example 4.2 Calculate the length of $[\bar{3}1\bar{2}]$ in a trigonal unit cell where $a =$ 0.473 nm and $\alpha = 51.22°$.

Using Eq. (4.9) and the scalar product equation, $r^2 = \mathbf{r} \cdot \mathbf{r} = U^2\ a^2 + V^2\ b^2 + W^2\ c^2 + 2VWbc\cos\alpha + 2WUca\cos\beta + 2UVab\cos\gamma$. But $a = b = c$ and $\alpha = \beta = \gamma$. Hence, $r^2 = a^2[(U^2 + V^2 + W^2) + 2\cos\alpha(VW + WU + UV)] =$ Evaluating, $r =$ 2.094 nm.

4.6 Law of rational intercepts: reticular density

When the faces of crystals are allocated Miller indices (indexed) in the simplest manner, the indices are small whole numbers; only occasionally does the index of crystal face exceed 5. The law of rational intercepts, also called the law of rational indices, embodies this result, and can be interpreted in terms of lattice theory.

Consider the projection of an orthorhombic lattice, shown in Fig. 4.17. The traces of the families of planes (100) , (110) and $(2\bar{3}0)$ are outlined in relation to the **a**, **b** projection of the primitive unit cell. It can be shown that as the Miller indices increase numerically, the reticular densities, D_R, that is, the number of lattice points per unit area, may be expected to decrease. In Fig. 4.17, the (100) planes are the most densely populated, $D_R = \dfrac{1}{ac}$; the (110) planes with $D_R = \dfrac{1}{c\sqrt{a^2 + b^2}}$ are less more densely populated, and the $(2\bar{3}0)$, with $D_R = \dfrac{1}{c\sqrt{9a^2 + 4b^2}}$, less densely still, and so on. The more densely populated planes are those of wider interplanar spacing d in a given material: d is proportional to the reticular density or to 1/reticular area.

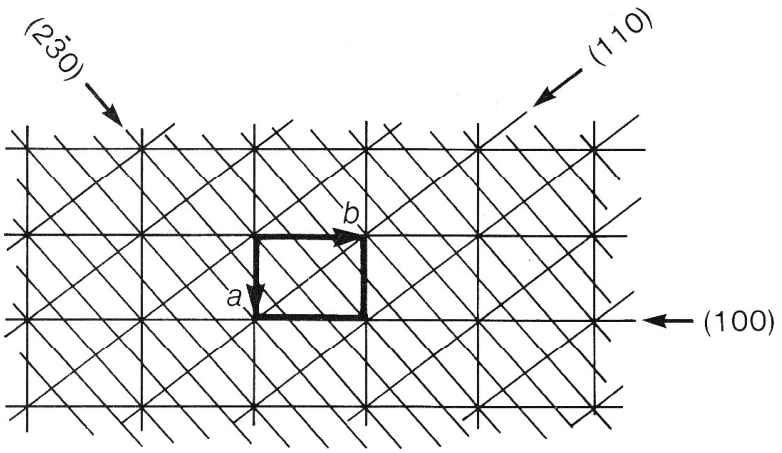

Fig. 4.17
The (100), (110) and (2$\bar{3}$0) families of planes in an orthorhombic lattice. [Reproduced by courtesy of Woodhead Publishing, UK.]

If a lattice is based on an orthorhombic C unit cell, $D_R(100)$ is the same as for the P cell although the interplanar spacing is halved, but $D_R(110)$ is now twice that in the P cell. If, for example, the unit dimensions are $a = 0.4, b = 0.6, c = 1.00$ nm, then the D_R ratios (100) : (110) : (2$\bar{3}$0) are 2.50 : 1.39 : 0.589. This topic further may be explored a little further, restricting the discussion to the cubic system. In this system

$$d(hkl) = \frac{1}{\sqrt{h^2 + k^2 + l^2}} \propto D_R \tag{4.11}$$

and there are the three lattices to consider, specified by P, I and F. The planes with the greater values of D_R would be expected to correspond to the more stable (lower energy) crystal state. Consider first a P unit cell; the D_R values are listed hereunder:

***P* unit cell**											
hkl	100	110	111	210	211	221	310	311	(222)	320	321
D_R	1	0.71	0.58	0.45	0.41	0.33	0.32	0.30	0.29	0.28	0.27

These data indicate a preference for the hexahedral (cubic) {100} form; sodium chlorate, which has a primitive unit cell, develops principally the forms {100}, {110} and {210}. Note that the *hkl* values listed are those found on an X-ray diffraction record. Morphologically, (222) is observed externally as (111) and, in general, $(2p)\,h, (2q)\,k$ and $(2r)\,l$ as $h\,k\,l$, where p, q and r are integers.

In an I unit cell, any index for which $h + k + l$ is not an even number is doubled, as underlined in the table, where the fundamental $h\,k\,l$ is written as a subscript:

***I* unit cell**											
hkl	$200_{(100)}$	110	$\underline{222}_{(111)}$	$\underline{420}_{(210)}$	211	$\underline{442}_{(221)}$	310	$\underline{622}_{(311)}$	$\underline{640}_{(320)}$	321	411
D_R	0.5	0.71	0.29	0.22	0.41	0.17	0.32	0.15	0.14	0.27	0.24

In this lattice, there is a preference for dodecahedral {110} forms, as in the garnets and the caesium halides, except caesium fluoride, which show also the {100} and {111} forms. Although caesium chloride, bromide and iodide do not have strictly *I* unit cells because the atom at the centre of the unit cell is different from those at its corners, they simulate *I* in their habits. Rewriting the morphological forms in order of importance:

$$110 > 100 > 211 > 310 > 111 > 321 > 411 > 210 > 221 > 311 > 320$$

For an *F* unit cell, any index not containing mixed odd and even integers is doubled, as in the following record:

	***F* unit cell**										
hkl	$\underline{200}_{(100)}$	$\underline{220}_{(110)}$	111	$\underline{420}_{(210)}$	$\underline{422}_{(211)}$	$\underline{442}_{(221)}$	$\underline{620}_{(310)}$	311	331	511	531
D_R	0.50	0.35	0.58	0.22	0.20	0.17	0.16	0.30	0.23	0.19	0.17

Here, a preference exists for octahedral {111} and {100} forms, as in diamond and calcium fluoride. Re-writing the morphological forms in order of importance:

$$111 > 100 > 110 > 311 > 331 > 210 > 211 > 221/511 > 531 > 310$$

In simple structures, component atoms often occupy positions on lattice points, so that the population of atoms on a given plane may be related in a simple manner to the reticular density. The faces on a crystal represent the terminations of families of planes, and a crystal grows in such a way that the external faces are planes of highest reticular density. This situation produces a more energetically stable system, because of a better balance of interatomic forces than would arise with a surface that contains, on the atomic scale, relatively large holes.

As the planes of higher reticular density are those of lower Miller indices, the law of rational intercepts follows logically; it was developed significantly by Bravais [3]. If the unit cells in a crystal pack in the manner of Fig. 4.18, the external faces will have rational indices. A crystal does not build in fractions of unit cells, so that the apparent steps shown here on {110} are only of atomic dimensions and will not be observed.

A more general discussion on crystal growth and form has been given by Donnay and Harker [6], who took space group symmetry into account. Thus, morphologically, quartz would be expected to have {0001} as the dominant form. In practice, this form is observed rarely. The first three D_R values are $(0001), (10\bar{1}0)$ and $(10\bar{1}1)$; but on account of the 3_1 screw axis in quartz, (0003) takes the place of (0001), so moving this plane down in the D_R order. Subsequent work defined a growth morphology [7, 8] that attempted to explain crystal growth in terms of an attachment energy of a crystal fragment on to an already formed crystal. Equilibrium morphology attempts to determine crystal growth in terms of minimum surface energy [9], the greater stability corresponding to low surface energy and high reticular density. A more recent publication [10] considers the morphology and growth of crystals in detail.

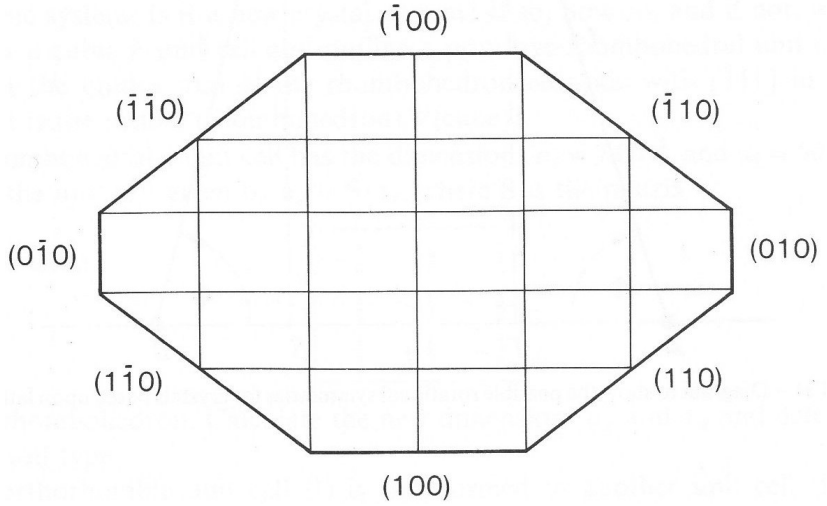

Fig. 4.18
Common shape of the cross-section on an orthorhombic crystal; the zone axis [001] is normal to the diagram. The {110} planes on the macroscopic have rational indices because the apparent steps are microscopic in size. [Reproduced by courtesy of Woodhead Publishing, UK.]

4.7 Reciprocal lattice

It is convenient to introduce here the concept of the reciprocal lattice, which will be needed when considering the diffraction of X-rays in a subsequent chapter. A reciprocal lattice exists for each of the Bravais lattices, and may be derived by the following construction, applied to a monoclinic *P* lattice.

A projection on to the (010) plane is shown in Fig. 4.19; the primitive unit cell is outlined by vectors **a** and **c**. Lines are constructed from the origin, *O*, and normal to the families of Bravais lattice planes shown. Recall that, in general, the normal to a lattice plane does not coincide with the direction of the same indices.

Along each line, reciprocal lattice points are defined such that the distances to these points from the origin are inversely proportional to the corresponding interplanar spacings. Thus, in Fig. 4.19, the families of planes (100), (101) and (001) give rise to reciprocal lattice points at distances from the origin that are proportional to $1/d(100), 1/d(101)$ and $1/d(001)$, where $d(100) = OP$, $d(101) = OQ$ and $d(001) = OR$. In general,

$$d^* = K/d(hkl) \tag{4.12}$$

where the parameter K is unity (see also Section 6.4ff). The vectors $\mathbf{d}^*(100)$, $\mathbf{d}^*(010)$ and $\mathbf{d}^*(001)$ may be taken to define the translation vectors $\mathbf{a}^*$, $\mathbf{b}^*$ and $\mathbf{c}^*$ of a unit cell in the reciprocal lattice, also termed the reciprocal unit cell. The following equations for the monoclinic reciprocal lattice can now be determined. From Eq. (4.12),

$$d^*(100) = 1/d(100) = a^* \tag{4.13}$$

But $d(100)$ is, from Fig. 4.19, $a \sin \beta$. Hence

$$a^* = 1/(a \sin \beta) \tag{4.14}$$

Similarly

$$c^* = 1/(c \sin \beta) \tag{4.15}$$

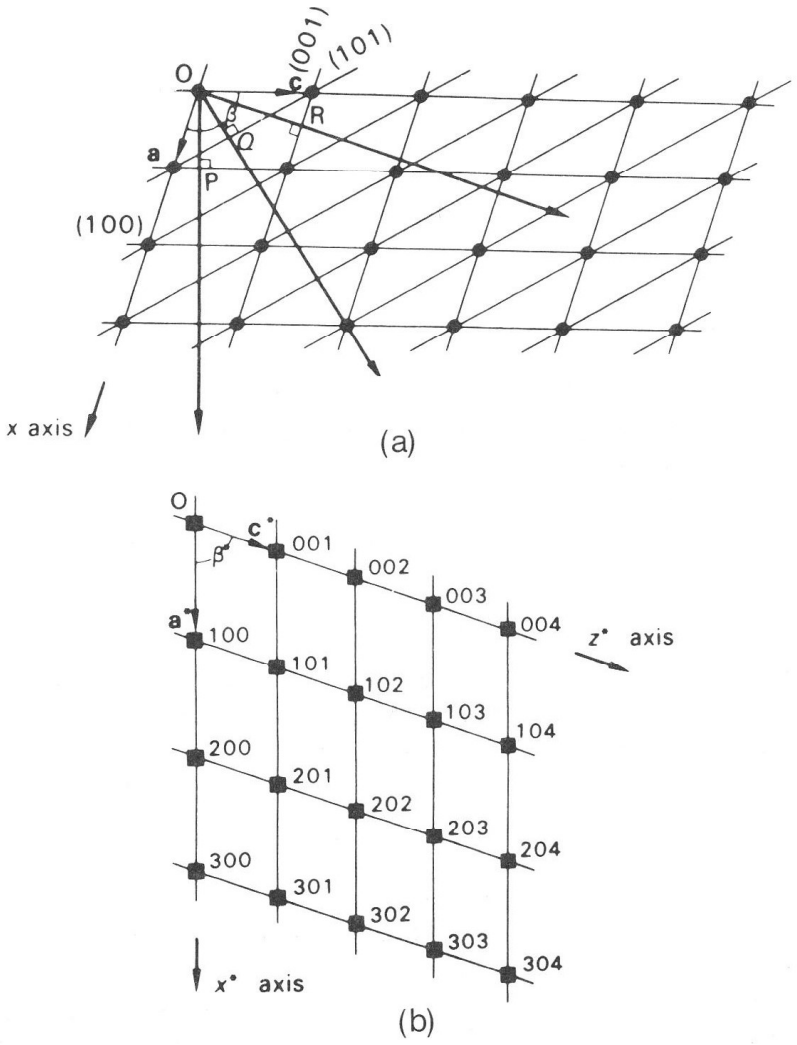

Fig. 4.19
Reciprocal lattice. (a) Monoclinic lattice in projection on to (010), showing P unit cells and the traces of the (100), (101) and (001) families of planes. (b) Monoclinic reciprocal lattice constructed from the lattice in (a), in projection on the a^*, c^* plane.

But

$$b^* = 1/b \tag{4.16}$$

because $d^*(010)$ is normal to the a, c plane. The unique β^* angle is given by

$$\beta^* = (180^\circ - \beta) \tag{4.17}$$

Furthermore,

$$\mathbf{a} \cdot \mathbf{a}^* = aa^* \cos \angle \mathbf{aa}^* = a(1/a)\cos(\beta - 90^\circ) = 1 \tag{4.18}$$

and similarly for $\mathbf{b} \cdot \mathbf{b}^*$ *and* $\mathbf{c} \cdot \mathbf{c}^*$. For the mixed products,

$$\mathbf{a} \cdot \mathbf{b} = ab^* \angle \cos \mathbf{ab}^* = 0 \tag{4.19}$$

and similarly for all other such products. The relationships in Eq. (4.18) and Eq. (4.19) apply to all crystal systems.

In looking next at the reciprocal lattice in a more general manner, the material in Appendix A3 will be useful. In Fig. 4.20, the z^* axis is normal to the plane a, b. Since $\mathbf{c} \cdot \mathbf{c}^* = 1 = cc^* \cos \angle COR$,

$$c^* = |\mathbf{c}^*| = 1/c \cos \angle COR \tag{4.20}$$

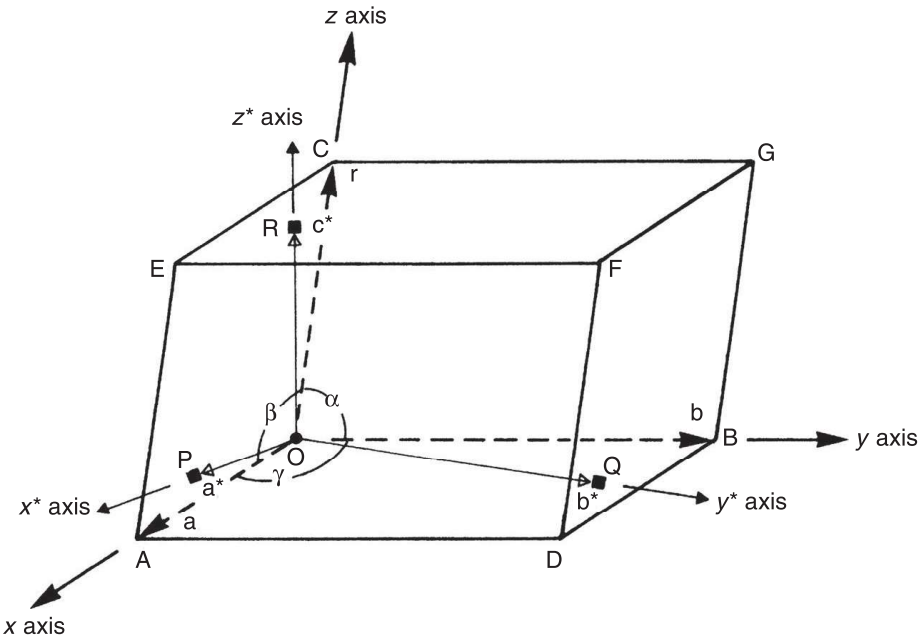

Fig. 4.20
Triclinic unit cell, with vectors **a**, **b** and **c**, and the corresponding reciprocal unit cell vectors $\mathbf{a}^*$, $\mathbf{b}^*$ and $\mathbf{c}^*$. [Reproduced by courtesy of Springer Science+Business Media, New York, © Kluwer Academic/Plenum Publishing.]

But $\mathbf{c}^*$ is normal to both **a** and **b**, so that it lies in the direction of their vector product. Hence,

$$\mathbf{c}^* = \eta(\mathbf{a} \times \mathbf{b}) \tag{4.21}$$

where η is a constant. From Appendix A3, $V = \mathbf{c}^* \cdot (\mathbf{a} \times \mathbf{b})$; forming next the scalar product of Eq. (4.21) and **c**,

$$\mathbf{c} \cdot \mathbf{c}^* = \eta \mathbf{c} \cdot (\mathbf{a} \times \mathbf{b}) = \eta V = 1$$

so that $\eta = \frac{1}{V}$; hence, from Eq. (4.21)

$$\mathbf{c}^* = \frac{(\mathbf{a} \times \mathbf{b})}{\mathbf{c} \cdot (\mathbf{a} \times \mathbf{b})} \tag{4.22}$$

and similarly for $\mathbf{a}^*$ and $\mathbf{b}^*$ by cyclic permutation. In scalar form,

$$c^* = |\,\mathbf{c}^*| = \frac{ab \sin \gamma}{V} \tag{4.23}$$

and similarly for a^* and b^* by cyclic permutation.

The angles of the reciprocal unit cell are obtained through Fig. 4.21. The z^* axis is perpendicular to the plane (001) and is, therefore, coincident with the pole of the great circle containing x and y. Similar arguments apply to x^* and y^*. Thus, the arc $B'C'$ is, at all points on it, 90° from the great circle of which AB is an arc; similarly with $B'C'$ and $C'A'$ *mutatis mutandis*. Hence, the triangle $A'B'C'$ is the polar triangle of triangle ABC.
Referring now to Section 2.6.1, it follows that

$$\gamma^* = 180^\circ - \angle C$$
$$\gamma \;\; = 180^\circ - \angle C'$$

with similar expressions for A, B', A and B'. Hence, from Eq. (2.33)

$$\cos \gamma^* = \frac{\cos \gamma + \cos \alpha \cos \beta}{\sin \alpha \sin \beta} \tag{4.24}$$

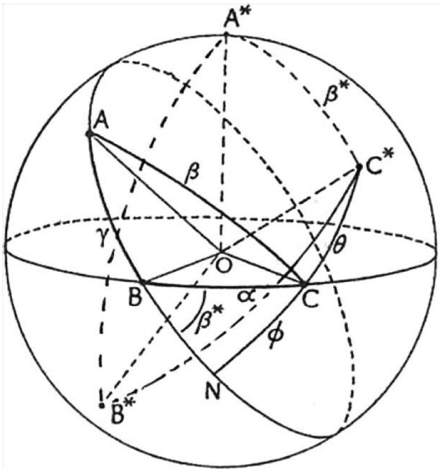

Fig. 4.21
Spherical triangle ABC and its polar triangle $A^*B^*C^*$. [Reproduced by courtesy of Springer Science+Business Media, New York, © Kluwer Academic/Plenum Publishing.]

since A, B and C are here identified with α, β and γ from Euler's construction (Section 3.6.3); the results for $\cos\alpha^*$ and $\cos\beta^*$ may be obtained by cyclic permutation. It remains to show that the reciprocal lattice points, as constructed here, form a true lattice.

From Eq. (A3.39), the vector normal to the plane $(h\,k\,l)$ is $h(\mathbf{b}\times\mathbf{c})+k(\mathbf{c}\times\mathbf{a})+l(\mathbf{a}\times\mathbf{b})$. Dividing by V, and denoting the resulting vector $\mathbf{d}^*(hkl)$,

$$\mathbf{d}^*(hkl)=\left\{h\frac{(\mathbf{b}\times\mathbf{c})}{\mathbf{a}\cdot(\mathbf{b}\times\mathbf{c})}+k\frac{(\mathbf{c}\times\mathbf{a})}{\mathbf{b}\cdot(\mathbf{c}\times\mathbf{a})}+l\frac{(\mathbf{a}\cdot\mathbf{b})}{\mathbf{c}\cdot(\mathbf{a}\cdot\mathbf{b})}\right\}=h\mathbf{a}^*+k\mathbf{b}^*+l\mathbf{c}^* \tag{4.25}$$

as given in Eq. (A3.5). Since h, k and l are integers, the vectors $\mathbf{d}^*(hkl)$ drawn from the common origin form a lattice, the reciprocal lattice, with translation vectors $\mathbf{a}^*$, $\mathbf{b}^*$ and $\mathbf{c}^*$ and interaxial angles

$$\left.\begin{aligned}\alpha^*&=\angle\mathbf{b}^*\mathbf{c}^*=\angle 010-001\\ \beta^*&=\angle\mathbf{c}^*\mathbf{a}^*=\angle 010-001\\ \gamma^*&=\angle\mathbf{a}^*\mathbf{b}^*=\angle 100-010\end{aligned}\right\} \tag{4.26}$$

It should be noted that reciprocal lattice points are denoted by the hkl values of the family of planes in the Bravais lattice from which they were derived, but are written without parentheses.

4.8 Rotational symmetry of lattices

Having now studied lattice geometry in some detail, it is relevant to show analytically that rotational symmetry in a periodic lattice is restricted to the degrees 1, 2, 3, 4 and 6, which was demonstrated graphically in Section 3.5.5.

In Fig. 4.22, A and B represent two adjacent points, of repeat distance t, in any row of a lattice, and an R-fold axis acts normal to the plane and through each lattice point. An R-fold anticlockwise rotation ϕ about the axis through A maps B on to B', and a similar but clockwise rotation about the axis through B maps A on to A'; it follows that $A'B'$ is parallel to AB. The lines $A'S$ and $B'T$ are drawn perpendicularly to the line AB. In a lattice, any two points in a row must be separated by an integral multiple of the repeat distance in

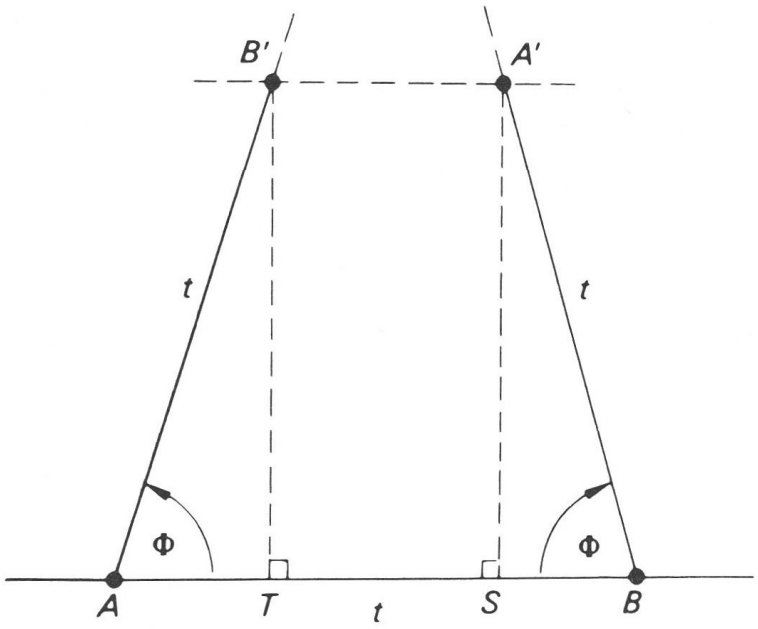

Fig. 4.22
Permitted rotational symmetries in lattices are 1–, 2–, 3–, 4 – and 6– fold, corresponding to rotations of 0° (360°), 180°, 120°, 90° and 60°.

the direction of that row. Thus, $A'B' = mt$, where m is an integer. Furthermore, $A'B' = t - (AT + BS) = t - 2t\cos\phi$; hence, $m = 1 - 2\cos\phi$, or

$$\cos\phi = (1 - m)/2 = M/2 \tag{4.27}$$

where M is another integer. Since $|\cos\phi| \leq 1$, the only values of M which are admissible are 2, –2, –1, 0 and 1, which correspond to rotations of 360°, 180°, 120°, 90° and 60°, respectively. This analysis provides a deeper meaning that that given earlier. An alternative proof, which depends upon the fact that the trace of a rotation symmetry matrix lies between –3 and +1, is described in Appendix A3.7.

The 14 Bravais lattices are presented in their entirety by Fig. 4.23. Can you now write the relationships between $a, b, c,$ and α, β, γ for each unit cell shown therein?

4.9 Lattice transformations

In practice, it is often necessary to transform the axes of the unit cell of a crystal that may have been first chosen by experiment. The parameters that may be involved, as well as the unit cell parameters a, b and c, are the Miller indices hkl, the zone symbols or directions UVW, the reciprocal unit cell parameters a^*, b^*, c^* and the coordinates x, y and z in the direct unit cell.

4.9.1 Bravais lattice unit cell vectors

Let $\mathbf{a}$, $\mathbf{b}$ and $\mathbf{c}$ be transformed to $\mathbf{a}'$, $\mathbf{b}'$ and $\mathbf{c}'$, such that

$$\begin{aligned} \mathbf{a}' &= s_{11}\mathbf{a} + s_{12}\mathbf{b} + s_{13}\mathbf{c} \\ \mathbf{b}' &= s_{21}\mathbf{a} + s_{22}\mathbf{b} + s_{23}\mathbf{c} \\ \mathbf{c}' &= s_{31}\mathbf{a} + s_{32}\mathbf{b} + s_{33}\mathbf{c} \end{aligned} \tag{4.28}$$

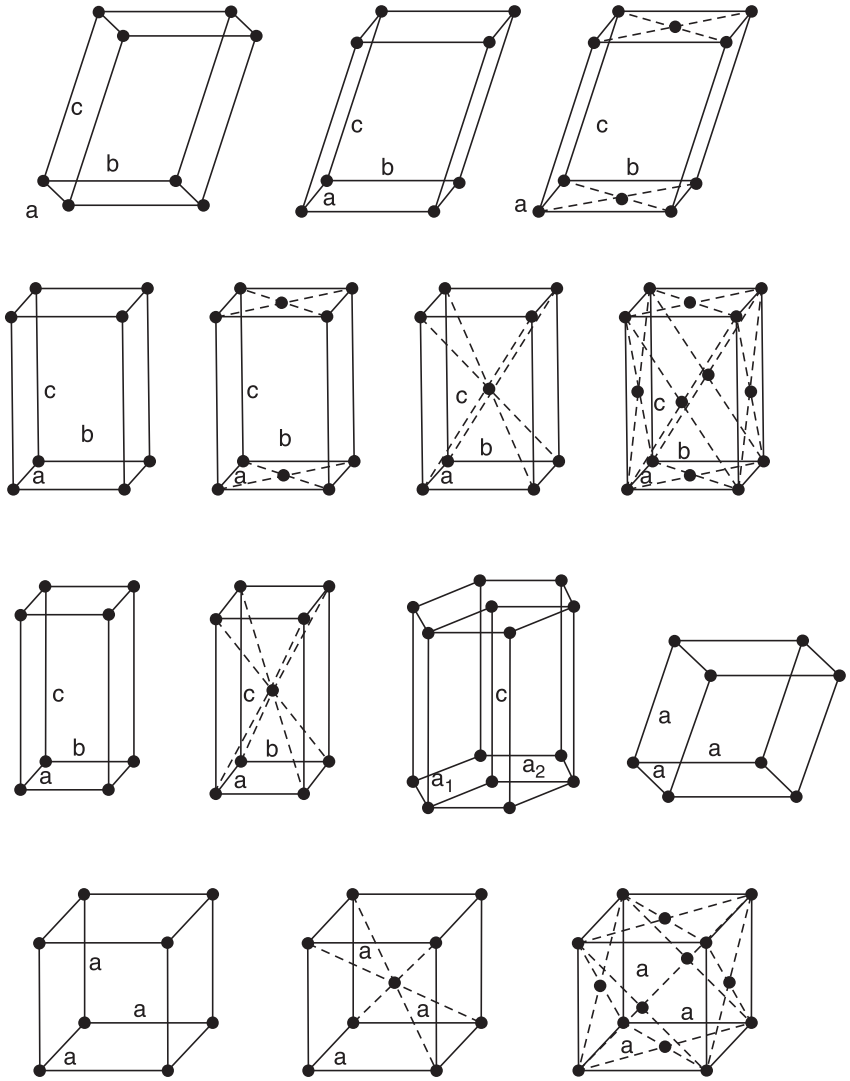

Fig. 4.23
The 14 Bravais lattices. In order, left–right, top–bottom: triclinic *P*, monoclinic *P*, monoclinic *C*, orthorhombic *P*, orthorhombic *C*, orthorhombic *I*, orthorhombic *F*, tetragonal *P*, tetragonal *I*, hexagonal *P* (three unit cells are shown), rhombohedral *R*, cubic *P*, cubic *I*, cubic *F*. [Reproduced by courtesy of Springer Science+Business Media, New York, © Kluwer Academic/Plenum Publishing.]

Following the matrix notation discussed in Appendix A3,

$$\begin{pmatrix} \mathbf{a}' \\ \mathbf{b}' \\ \mathbf{c}' \end{pmatrix} = \begin{pmatrix} s_{11} & s_{12} & s_{13} \\ s_{21} & s_{22} & s_{23} \\ s_{31} & s_{32} & s_{33} \end{pmatrix} \begin{pmatrix} \mathbf{a} \\ \mathbf{b} \\ \mathbf{c} \end{pmatrix} \tag{4.29}$$

or concisely

$$\mathbf{a}' = \mathbf{S}\,\mathbf{a} \tag{4.30}$$

where $\mathbf{a}'$ and $\mathbf{a}$ represent the two column vectors and $\mathbf{S}$ the matrix of elements s_{ij}. The inverse transformation may be written

$$\mathbf{a} = \mathbf{S}^{-1}\,\mathbf{a}' \tag{4.31}$$

where $\mathbf{S}^{-1}$ is the inverse matrix to $\mathbf{S}$. The elements of the inverse matrix, denoted s_{ij}^{-1}, obtained as

$$s_{ij}^{-1} = \frac{1}{\det(\mathbf{S})}(-1)^{i+j}|M_{ji}|$$

where $|M_{ji}|$ is the *minor* determinant of $\mathbf{S}$, obtained by striking the row and column containing the ***ji*** element (Appendix A3.4.10). If the matrix is

$$\mathbf{S} = \begin{pmatrix} \frac{2}{3} & \frac{1}{3} & \frac{1}{3} \\ \frac{1}{3} & \frac{1}{3} & \frac{1}{3} \\ \frac{1}{3} & \frac{2}{3} & \frac{1}{3} \end{pmatrix}$$

the value of det($\mathbf{S}$) may be obtained as described in Appendix A3, or more quickly from the cross-multiplication rule:

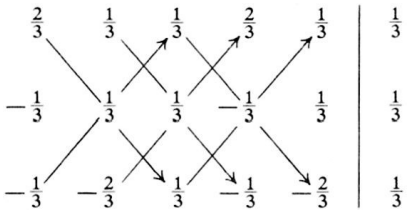

whence

$$\det(\mathbf{S}) = \frac{2}{27} - \frac{1}{27} + \frac{2}{27} + \frac{1}{27} + \frac{4}{27} + \frac{1}{27} = \frac{1}{3}$$

The element s_{23}, for example, of the inverse matrix can be evaluated from $\mathbf{S}$ as:

$$s_{23}^{-1} = \frac{1}{1/3}(-1)^{2+3}|M_{32}| = \frac{(-1)^{2+3}}{1/3}\begin{vmatrix} \frac{2}{3} & \frac{1}{3} \\ \frac{1}{3} & \frac{1}{3} \end{vmatrix} = \frac{1}{1/3}(-1)\,(1/3) = -1$$

In this way, the inverse matrix can be built up:

$$\mathbf{S}^{-1} = \begin{pmatrix} 1 & \bar{1} & 0 \\ 0 & 1 & \bar{1} \\ 1 & 1 & 1 \end{pmatrix}. \tag{4.32}$$

4.9.2 Zone symbols and lattice directions

It will have been noticed that the normals to faces $(h\,k\,l)$ in the construction of the stereographic projection are also the directions of vectors to points *hkl* in the reciprocal lattice: they are both normals to lattice planes. The difference lies in the fact that in the stereographic projection the normals lack the linear measurement explicit in the reciprocal lattice.

A direction $\mathbf{r}$ in a direct unit cell may be written as

$$\mathbf{r} = U\mathbf{a} + V\mathbf{b} + W\mathbf{c} \tag{4.33}$$

and in a transformed cell as

$$\mathbf{r} = U'\mathbf{a}' + V'\mathbf{b}' + W'\mathbf{c}' \tag{4.34}$$

From Eq. (4.33) and Eq. (4.34)

$$(U'V'W')\begin{pmatrix} \mathbf{a}' \\ \mathbf{b}' \\ \mathbf{c}' \end{pmatrix} = (U\ V\ W)\begin{pmatrix} \mathbf{a} \\ \mathbf{b} \\ \mathbf{c} \end{pmatrix} = (U\,V\,W)\,\mathbf{S}^{-1}\begin{pmatrix} \mathbf{a}' \\ \mathbf{b}' \\ \mathbf{c}' \end{pmatrix}$$

or

$$(U'V'W') = (U\,V\,W)\mathbf{S}^{-1}$$

Hence, from Appendix A3.4.12, and concisely,

$$\mathbf{U}' = \mathbf{U}\mathbf{S}^{-1} = (\mathbf{S}^{-1})^{\mathrm{T}}\mathbf{U} \tag{4.35}$$

where $\mathbf{U}$ and $\mathbf{U}'$ are now column vectors.

Since $(\mathbf{S}^{-1})^{\mathrm{T}} = (\mathbf{S}^{\mathrm{T}})^{-1}$, pre-multiplication of both sides of Eq. (4.35) by $\mathbf{S}^{\mathrm{T}}$ leads to,

$$\mathbf{S}^{\mathrm{T}}\mathbf{U}' = \mathbf{S}^{\mathrm{T}}(\mathbf{S}^{\mathrm{T}})^{-1}\mathbf{U} = \mathbf{U}$$

or

$$\mathbf{U} = \mathbf{S}^{\mathrm{T}}\mathbf{U}' \tag{4.36}$$

4.9.3 Coordinates of points in the direct unit cell

For any fractional coordinate x, y, z in the unit cell

$$\mathbf{r} = x\mathbf{a} + y\mathbf{b} + z\mathbf{c}$$

From the transformation in Section 4.9.2, it is evident that these coordinates transform as do zone symbols. Thus,

$$\mathbf{x}' = (\mathbf{S}^{-1})^{\mathrm{T}}\mathbf{x} \tag{4.37}$$

and

$$\mathbf{x} = \mathbf{S}^{\mathrm{T}}\mathbf{x}' \tag{4.38}$$

4.9.4 Miller indices

From Eq. (4.25) and EQ. (4.33),

$$\mathbf{d}^*(hkl) \cdot \mathbf{r} = hU + kV + lW$$

and following Eq. (4.36)

$$\mathbf{d}^*(hkl) \cdot \mathbf{r} = (h \quad k \quad l)\begin{pmatrix} U \\ V \\ W \end{pmatrix} = (h \quad k \quad l)\,\mathbf{S}^{\mathrm{T}}\begin{pmatrix} U' \\ V' \\ W' \end{pmatrix}$$

But in terms of the transformed cell,

$$\mathbf{d}^*(hkl) \cdot \mathbf{r} = \begin{pmatrix} h' & k' & l' \end{pmatrix}\begin{pmatrix} U' \\ V' \\ W' \end{pmatrix}$$

and because $\mathbf{d}^*(hkl)$ and $\mathbf{d}^*(h'k'l')$ are one and the same vector.

$$\begin{pmatrix} h' & k' & l' \end{pmatrix} = (h \quad k \quad l)\,\mathbf{S}^{\mathrm{T}}$$

Transposing, as before

$$\begin{pmatrix} h' \\ k' \\ l' \end{pmatrix} = \mathbf{S}\begin{pmatrix} h \\ k \\ l \end{pmatrix}$$

or

$$\mathbf{h}' = \mathbf{S}\,\mathbf{h} \tag{4.39}$$

By multiplying by $\mathbf{S}^{-1}$,

$$\mathbf{h} = \mathbf{S}^{-1}\mathbf{h}' \tag{4.40}$$

where $\mathbf{h}$ and $\mathbf{h}'$ represent h, k, l and h', k', l'; thus, the Miller indices transform as do unit cell vectors. Miller–Bravais indices transform as Miller indices, using h, k and l from the h, k, i and l values.

4.9.5 Reciprocal unit cell vectors

Equation (4.25) may be written as

$$\mathbf{d}^*(hkl) = \left(\mathbf{a}^* \;\; \mathbf{b}^* \;\; \mathbf{c}^*\right)\mathbf{S}^{-1}\begin{pmatrix} h' \\ k' \\ l' \end{pmatrix}.$$

In the new reciprocal cell

$$\mathbf{d}^*(hkl) = \left(\mathbf{a}^{*\prime} \;\; \mathbf{b}^{*\prime} \;\; \mathbf{c}^{*\prime}\right)\begin{pmatrix} h' \\ k' \\ l' \end{pmatrix}$$

so that

$$\left(\mathbf{a}^{*\prime} \;\; \mathbf{b}^{*\prime} \;\; \mathbf{c}^{*\prime}\right) = \left(\mathbf{a}^* \;\; \mathbf{b}^* \;\; \mathbf{c}^*\right)\mathbf{S}^{-1}$$

By transposition, as earlier

$$\mathbf{a}^{*\prime} = (\mathbf{S}^{-1})^{\mathrm{T}}\mathbf{a}^* \tag{4.41}$$

and

$$\mathbf{a}^* = \mathbf{S}^{\mathrm{T}}\mathbf{a}^{*\prime} \tag{4.42}$$

so that reciprocal unit cell vectors transform as do zone symbols and coordinates in a unit cell of a Bravais lattice. These transformations are summarized in Table 4.5

Table 4.5 Relationships among transformation matrices.

Matrix S	**Matrix $\mathbf{S}^{-1}$**
Old unit cell translation vectors to new	New unit cell translation vectors to old
Old Miller indices to new	New Miller indices to old
Matrix $(\mathbf{S}^{-1})^{\mathbf{T}}$	**Matrix $\mathbf{S}^{\mathbf{T}}$**
Old reciprocal unit cell translation vectors to new	New reciprocal unit cell translation vectors to old
Old zone symbols to new	New zone symbols to old
Old Bravais unit cell coordinates to new	New Bravais unit cell coordinates to old

4.9.6 Volume relationships

It has been shown earlier that $V = \mathbf{a} \cdot (\mathbf{b} \times \mathbf{c})$. Thus, it follows from Eq. (4.30) that the volume V' of the transformed cell is given by

$$V' = \det(\mathbf{S})V \tag{4.43}$$

Thus, for the matrix

$$\mathbf{S} = \begin{pmatrix} 2/3 & 1/3 & 1/3 \\ 1/3 & 1/3 & 1/3 \\ 1/3 & 2/3 & 1/3 \end{pmatrix}$$

which applies to the transformation $\mathbf{a}\,(\text{rhombohedral}, R_{\text{obv}}) \rightarrow \mathbf{a}\left(\text{hexagonal}, H_{\text{triply primitive}}\right), \det(\mathbf{S}) = 1/3$, so that $V_{\text{R}} = 1/3 V_{\text{H}}$, which is the expected result for the relationship between the triply primitive hexagonal and rhombohedral unit cells.

4.9.7 Reciprocity of *F* and *I* unit cells

In Fig. 4.24, a primitive unit cell has been selected from the face centered unit cell by the transformation

$$\begin{aligned} \mathbf{a}_P &= \frac{1}{2}\mathbf{b}_F + \frac{1}{2}\mathbf{c}_F \\ \mathbf{b}_P &= \frac{1}{2}\mathbf{c}_F + \frac{1}{2}\mathbf{a}_F \\ \mathbf{c}_P &= \frac{1}{2}\mathbf{a}_F + \frac{1}{2}\mathbf{b}_F \end{aligned} \tag{4.44}$$

From Section 4.7, with appropriate cyclic permutation

$$\begin{aligned} \mathbf{a}_P^* = (\mathbf{b}_P \times \mathbf{c}_P)/V_P &= \left[\left(\frac{1}{2}\mathbf{c}_F + \frac{1}{2}\mathbf{a}_F\right) \times \left(\frac{1}{2}\mathbf{a}_F + \frac{1}{2}\mathbf{b}_F\right)\right]/V_P \\ &= \frac{1}{4}[(\mathbf{c}_F \times \mathbf{b}_F) + (\mathbf{c}_F \times \mathbf{a}_F) + (\mathbf{a}_F \times \mathbf{b}_F)]/V_F \\ &= \frac{c_F b_F}{V_F}\sin\alpha + \frac{c_F a_F}{V_F}\sin\beta + \frac{a_F b_F}{V_F}\sin\gamma \end{aligned}$$

since $V_F = 4V_P$. Hence,

$$\mathbf{a}_P^* = -\mathbf{a}_F^* + \mathbf{b}_F^* + \mathbf{c}_F^* \tag{4.45}$$

with similar expressions for $\mathbf{b}_P^*$ and $\mathbf{c}_P^*$. The negative sign in front of $\mathbf{a}_F^*$ in Eq. (4.45) is needed in order to preserve right-handed axes from the product $(\mathbf{c}_F \times \mathbf{b}_F)$.

In the case of the body-centered unit cell, the equations similar to Eq. (4.44) are

$$\mathbf{a}_P = -\frac{1}{2}\mathbf{a}_I + \frac{1}{2}\mathbf{b}_I + \frac{1}{2}\mathbf{c}_I \tag{4.46}$$

with similar expressions for $\mathbf{b}_P$ and $\mathbf{c}_P$. By writing Eq. (4.45) as

$$\mathbf{a}_P^* = -2\mathbf{a}_F^*/2 + 2\mathbf{b}_F^*/2 + 2\mathbf{c}_F^*/2 \tag{4.47}$$

it follows that an *F* unit cell in a Bravais lattice reciprocates into an *I* unit cell in the corresponding reciprocal lattice, where the *I* unit cell is defined by the

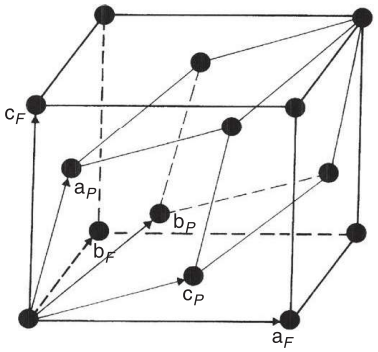

Fig. 4.24
Cubic *F* unit cell with an inscribed rhombohedron.

vectors $2\mathbf{a}_F^*$, $2\mathbf{b}_F^*$ and $2\mathbf{c}_F^*$. If, as is customary in practice, the reciprocal of an I unit cell is defined by vectors $\mathbf{a}_F^*$, $\mathbf{b}_F^*$ and $\mathbf{c}_F^*$, then only those reciprocal lattice points for which each of $h+k, k+l$ (and $l+h$) are even integers belong to the reciprocal of the I unit cell. In other words, Bragg reflections from an F unit cell have indices of the same parity (see also Section 6.6.3).

Example 4.3 A tetragonal C unit cell with $a = 4.774$ and $c = 8.361$ is transformed to a tetragonal P. Calculate the new unit cell dimensions and the position of a point $(0.411, -0.607, -0.193)$ in the new, C unit cell.

The transformation matrix is $\begin{pmatrix} \frac{1}{2} & -\frac{1}{2} & 0 \\ \frac{1}{2} & \frac{1}{2} & 0 \\ 0 & 0 & 1 \end{pmatrix}$ and the inverse matrix is $\begin{pmatrix} 1 & 1 & 0 \\ \bar{1} & 1 & 0 \\ 0 & 0 & 1 \end{pmatrix}$.

Thus, the P unit cell dimensions are $a' = b' = 3.376, c' = 8.361$ Å, and the coordinates are $1.018\ (\equiv 0.018), -0.196, -0.193$. (The transpose of the inverse is required here.) The results may be checked by a scaled drawing.

4.9.8 Wigner–Seitz cells

Before leaving the topic of lattices and unit cells, it may be noted that any lattice can be represented by a true primitive unit cell, such cells being capable of being stacked by three-dimensional translations so as to generate the lattice from which they were derived. Conventional unit cells are chosen so that the symmetries of their lattices are always self-evident. However, it may be desirable in some solid state studies to work with a primitive unit cell, whatever the corresponding Bravais unit cell might be. Such a cell is the Wigner–Seitz, or Voronoi, cell, the construction of which from a body centred cubic unit cell is shown to be relatively straightforward, as follows.

In a cubic I unit cell, lines are drawn from a lattice point to its nearest neighbour lattice points. Planes are then constructed so as to bisect these lines perpendicularly and the planes then extended as necessary to form the closed polyhedron of smallest volume. In the case of the cubic I cell, the polyhedron is a truncated octahedron (Fig. 4.25a); the directions **a**, **b** and **c** are clearly the normals to {100}, whereas the normals to the hexagonal shaped faces are the directions <111>. For a cubic F cell, the Wigner–Seitz cell is a rhombic dodecahedron. These results are not surprising because the coordination numbers in body- and face-centred structures of identical species are eight and twelve respectively. Fig. 4.25b shows space filled by stacking equal Wigner–Seitz unit cells; each cell displays the full rotation symmetry of its lattice.

A similar type of construction in reciprocal space, or $\boldsymbol{k}$ space, produces the first Brillouin zone, of which there are twenty-four such zones. In some systems more than one Wigner–Seitz cell exist for each Bravais lattice because the shape of the Wigner–Seitz cell can depend also on the axial ratios; thus, in the tetragonal system, for example, two Wigner–Seitz cells are derived from the body centred lattice according as c/a is greater than or less than unity [11].

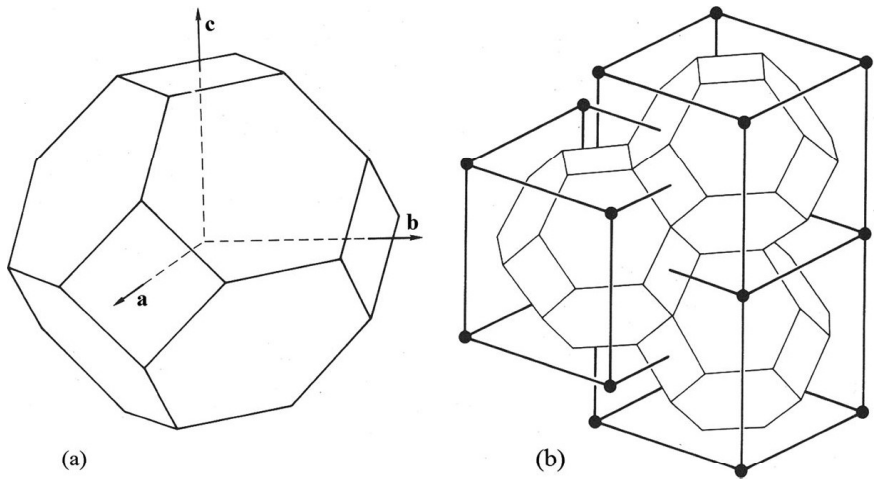

Fig. 4.25
(a) Wigner–Seitz (primitive) unit cell from a cubic lattice represented by an I unit cell; in reciprocal space, it corresponds to the first Brillouin zone. (b) Stacking of Wigner–Seitz cells to fill space. [Burns G and Glazer AM. *Space groups for solid state scientists*. 1978; reproduced by courtesy of Elsevier.]

The first Brillouin zone derived from an I unit cell is the Wigner–Seitz cell of an F unit cell lattice, illustrating again the reciprocity property of I and F unit cells. Brillouin zones are important in chemistry in the movement from bonds to bands in the quantum mechanical theory of metals [12], and in the physics of lattice dynamics [13]. The working advantage of the Wigner–Seitz cell lies in dealing with the smallest possible number of atoms while maintaining the full symmetry of the structure.

References 4

[1] Smith WF. *The Bravais lattices song*. 2002. [Tune: 'I am the Very Model of a Modern Major General', Gilbert WS and Sullivan A. *Pirates of Penzance*. 1880].
[2] Frankenheim ML. *Nova Acta Acad. Nat. Curr*. 1842; 9: 47.
[3] Bravais A. *Mem. Acad. Roy. Sci. France* 1846; 9: 255.
[4] Bravais A. *J. École Politech*. 1850; 19: 1, 127; 20: 102, 197.
[5] Ladd MFC. *J. Chem. Educ*. 1997; 74: 461.
[6] Donnay JHD and Harker D. *Amer. Mineral*. 1937; 22: 463.
[7] Berkovutch-Yellin Z. *J. Am. Chem. Soc*., 1985; 107: 8239.
[8] Docherty R, et al. *Phys. D: Appl. Phys*. 1991; 24: 89.
[9] Gibbs JW. *Collected works*. Longmans: 1928.
[10] Sunagawa I. *Crystals: growth, morphology and perfection*. Cambridge University Press: 2005.
[11] Burns G and Glazer AM. *Space groups for solid state scientists*. Elsevier: 2013.
[12] Altmann SL. *Band theory of metals*. Oxford Science Publications: 1970.
[13] Dove MT. *Introduction to lattice dynamics*. Cambridge University Press: 2005.

Problems 4

4.1 Consider two nets: (i) $a = b, \gamma = 90°$, and (ii) $a = b, \gamma = 120°$, (a) What is the plane point group symmetry at each lattice point? (b) To what two-dimensional system does each belong? (c) What is the result of centring the cell in each case? Give transformation matrices as appropriate.

4.2 To what crystal system does a unit cell belong if $a = 0.7, b = 0.6, c = 0.5\ nm, \alpha = 90°, \beta = 120°, \gamma = 90°$? Calculate the length of [123].

4.3 Define Bravais lattice. Which of the following unit cells represent a lattice: (i) Orthorhombic B, (ii) Tetragonal A, (iii) Triclinic I, (d) Cubic $B + C$?

4.4 What are the transformation equations for each of the following?
(a) Monoclinic $I \rightarrow$ Monoclinic C
(b) Rhombohedral $F \rightarrow$ Rhombohedral R
(c) Tetragonal $C \rightarrow$ Tetragonal P

4.5 Do the relationships $a \not= b \not= c, \alpha \not= \beta \not= 90^\circ, \gamma = 90^\circ$ represent a diclinic system? If so, how so, and if not, why not.

4.6 Outline an R cell within an F cubic unit cell such that their [111] directions coincide. What is the ratio $\frac{V_F}{V_R}$?

4.7 A rhombohedral I unit cell has the dimensions $\alpha = 7.000$ Å and $\alpha = 50.00^\circ$. Show that the cell obtained by the transformation $\mathbf{a}_R = \mathbf{S}\,\mathbf{a}_I$ is a rhombohedron and calculate its unit cell dimensions; the transformation matrix $\mathbf{S}$ is given by

$$\begin{pmatrix} -1/2 & 1/2 & 1/2 \\ 1/2 & -1/2 & 1/2 \\ 1/2 & 1/2 & -1/2 \end{pmatrix}$$

4.8 An orthorhombic unit cell I is transformed to another unit cell II by the equation $\mathbf{a}_{II} = \mathbf{S}\mathbf{a}_I$, where $\mathbf{S}$ is the matrix

$$\begin{pmatrix} 1 & \bar{1} & 0 \\ 1 & 1 & 0 \\ 0 & 0 & 1 \end{pmatrix}$$

What is the volume of cell II in terms of the volume of cell I? Hence, or otherwise, determine the coordinates of the point $(0.123, -0.671, 0.314)$ when transformed from cell I to cell II.

4.9 What are the relative reticular densities of the planes $(100), (220), (1\bar{3}0)$ and (042) in a cubic I unit cell? Which planes would be expected to form the external faces of a crystal that crystallizes with an I unit cell?

4.10 The monoclinic unit cell of gypsum has been determined in different ways:

	a/Å	b/Å	c/Å	β/°
(I)	10.51	15.15	6.545	151.72
(II)	5.669	15.15	6.545	118.58
(III)	10.51	15.15	6.285	99.30

(a) Outline the three unit cells on a common origin, projected on to the plane (010); a suitable scale is 10 mm = 1 Å.
(b) If cell I is P: (i) What are types II and III? (ii) What are the ratios $\frac{V_{III}}{V_{II}}$ and $\frac{V_{III}}{V_I}$? (iii) Which unit cell would you choose? Give reasons.
(c) Derive the matrices for the transformations from cell I to cell II, cell I to cell III and cell II to cell III.
(d) What are the dimensions of the reciprocal unit cell of the cell that you have chosen?
(e) Carry out the following transformations. (i) $(132)_I \rightarrow (hkl)_{III}$. (ii) $[21\bar{3}]_{II} \rightarrow [UVW]_{III}$. (iii) $(0.600,\ 0.500,\ -0.300)_{III} \rightarrow (x, y, z)_I$

4.11 Most elemental metals crystallize in a close packed cubic, close packed hexagonal or body centred cubic structure. Determine the packing fraction, or space occupied, by equal, spherical atoms in each structures.

4.12 A unit cell of a lattice has a single $\bar{4}$ axis along c. Show that the conditions $a = b \not= c$, and $\alpha = \beta = \gamma = 90^\circ$ must obtain.